Journal of
Medicinal Chemistry

Article

(*S*)-4-(Difluoromethyl)-5-(4-(3-methylmorpholino)-6-morpholino-1,3,5-triazin-2-yl)pyridin-2-amine (PQR530), a Potent, Orally Bioavailable and Brain Penetrable Dual Inhibitor of Class I PI3K and mTOR Kinase

Denise Rageot, Thomas Bohnacker, Erhan Keles, Jacob A. McPhail, Reece M. Hoffmann, Anna Melone, Chiara Borsari, Rohitha Sriramaratnam, Alexander Markus Sele, Florent Beaufils, Paul Hebeisen, Doriano Fabbro, Petra Hillmann, John E. Burke, and Matthias P. Wymann

J. Med. Chem., **Just Accepted Manuscript** • DOI: 10.1021/acs.jmedchem.9b00525 • Publication Date (Web): 07 Jun 2019

Just Accepted

is published by the American Chemical Society. 1155 Sixteenth Street N.W., Washington, DC 20036

(*S*)-4-(Difluoromethyl)-5-(4-(3-methylmorpholino)-6-morpholino-1,3,5-triazin-2-yl)pyridin-2-amine (PQR530), a Potent, Orally Bioavailable and Brain Penetrable Dual Inhibitor of Class I PI3K and mTOR Kinase

Denise Rageot,[†$] Thomas Bohnacker,[†$] Erhan Keles,[†] Jacob A. McPhail,[§] Reece M. Hoffmann,[§] Anna Melone,[†] Chiara Borsari,[†] Rohitha Sriramaratnam,[†] Alexander M. Sele,[†] Florent Beaufils,[†] Paul Hebeisen,[‡] Doriano Fabbro,[‡] Petra Hillmann,[‡] John E. Burke,[§] Matthias P. Wymann[†,*]

[†]Department of Biomedicine, University of Basel, Mattenstrasse 28, 4058 Basel, Switzerland;

[§]Department of Biochemistry and Microbiology, University of Victoria, Victoria, British Columbia BC V8W 2Y2, Canada

[‡]PIQUR Therapeutics AG, Hochbergerstrasse 60C, 4057 Basel, Switzerland;

[$]**Equal contribution**: these authors have contributed equally.

*Correspondence to: matthias.wymann@unibas.ch, Dept. Biomedicine, University of Basel, Mattenstrasse 28, 4058 Basel, Switzerland; Tel. +41 61 207 5046; Fax. +41 61 207 3566

KEYWORDS

Phosphoinositide 3-kinase (PI3K), mammalian or mechanistic target of rapamycin (mTOR); PI3K inhibitor, mTOR kinase inhibitor; brain penetrable; cancer; ATP-competitive; rapamycin, rapalogs, pharmacology, pharmacodynamics, clinical candidate

ABSTRACT

The phosphoinositide 3-kinase (PI3K)/mechanistic target of rapamycin (mTOR) pathway is frequently overactivated in cancer, and drives cell growth, proliferation, survival and metastasis. Here, we report a SAR-study which led to the discovery of a drug-like ATP-site PI3K/mTOR kinase inhibitor: (*S*)-4-(difluoromethyl)-5-(4-(3-methylmorpholino)-6-morpholino-1,3,5-triazin-2-yl)pyridin-2-amine (PQR530, compound **6**), which qualifies as a clinical candidate due to its potency and specificity for PI3K and mTOR kinases, and its pharmacokinetic properties, including brain penetration. Compound **6** showed excellent selectivity over a wide panel of kinases and an excellent selectivity against unrelated receptor enzymes and ion channels. Moreover, compound **6** prevented cell growth in a cancer cell line panel. The preclinical *in vivo* characterization of compound **6** in an OVCAR-3 xenograft model demonstrated good oral bioavailability, excellent brain penetration, and efficacy. Initial toxicity studies in rats and dogs qualify **6** for further development as a therapeutic agent in oncology.

INTRODUCTION

The phosphoinositide 3-kinase (PI3K) – mechanistic target of rapamycin (mTOR) signaling pathway plays a fundamental role in cell proliferation, growth, and survival. Aberrant activation of this signaling pathway has been shown to drive the progression of malignant tumors, which can be triggered by mutated growth factor receptors, PI3K, loss of PTEN (phosphatase and tensin homolog on chromosome 10) and effector proteins such as Ras.[1–3] The resulting increase of cellular PtdIns(3,4,5)P_3 subsequently recruits protein kinase B (PKB/Akt), which is fully activated by phosphorylation by phosphoinositide-dependent kinase 1 (PDK1) and the TOR complex 2 (TORC2) kinase at the plasma membrane.[4] By the phosphorylation of tuberous sclerosis 2 (TSC2, tuberin), PKB/Akt initiates the activation and assembly of TORC1 on endomembranes. TORC1 then augments cellular protein and lipid production *via* phosphorylation of S6 kinase (S6K). While TORC1 affects endomembrane dynamics and autophagy, TORC2 impacts on metabolic, cell cycle and cytoskeletal changes.[3]

Drugs targeting the pathway at multiple nodes, such as the first dual PI3K/mTOR inhibitor BEZ235 (dactolisib),[5,6] have provided promising preclinical results attenuating tumor growth driven specifically

by overactivated PI3K,[7] but also block growth of cancer cells with multiple activated pathways, such as in melanoma.[5] Although subsequent clinical studies of BEZ235 were plagued by adverse effects,[8] dual PI3K/mTOR inhibitors are still considered a valuable asset in cancer therapy, and are pursued in clinical trials.[2]

Recently, we presented PQR309 (bimiralisib, **5**)[9,10] as a novel, brain-penetrant pan-PI3K inhibitor, which also moderately targets mTOR kinase activity (Figure 1). First clinical results for **5** have been released,[15] and the compound is currently in phase II clinical trials. To maximize potency, we focused on the development of a brain permeant follow-up compound with a major enhancement in mTOR kinase inhibition.

We analyzed the activity profiles of compounds with a similar structure and binding mode as for **5**, and assessed their *in vitro* dissociation constants (K_d) for class I PI3K isoforms (α, β, γ, and δ) and mTOR. A selection of relevant clinical compounds is depicted in Figure 1 (for data see Table S1 in Supporting Information), and affinities for individual PI3K isoforms and mTOR provided a lead for novel compounds. Compound **1** (alpelisib, BYL719) has been reported as a specific PI3Kα inhibitor[12], but displayed in our hands only 7-fold selectivity over PI3Kγ, while sparing PI3Kβ, PI3Kδ and mTOR (> 250-fold). Pictilisib (GDC0941, **4**)[13] is a potent pan class I inhibitor that strongly binds to PI3Kα, β, and δ, with less affinity to PI3Kγ, however, its affinity to mTOR is >50-fold reduced compared to p110α. All other compounds are to various degrees dual class I PI3K [PI3K isoforms (α, β, γ, and δ)] and mTOR kinase inhibitors: **2** (buparlisib, BKM120),[9,14] **5**,[9–11,15] and **3** (apitolisib, GDC0980)[13], which all target class I as well as mTOR. Compound **6** emerging from the study presented here is a sub-nanomolar inhibitor of PI3Kα and mTOR, and targets other class I PI3Ks at around 10 nM (Table S1). Here, we report the lead optimization process using **5** as a starting template to generate **6**, a potent and brain-penetrant clinical candidate compound.

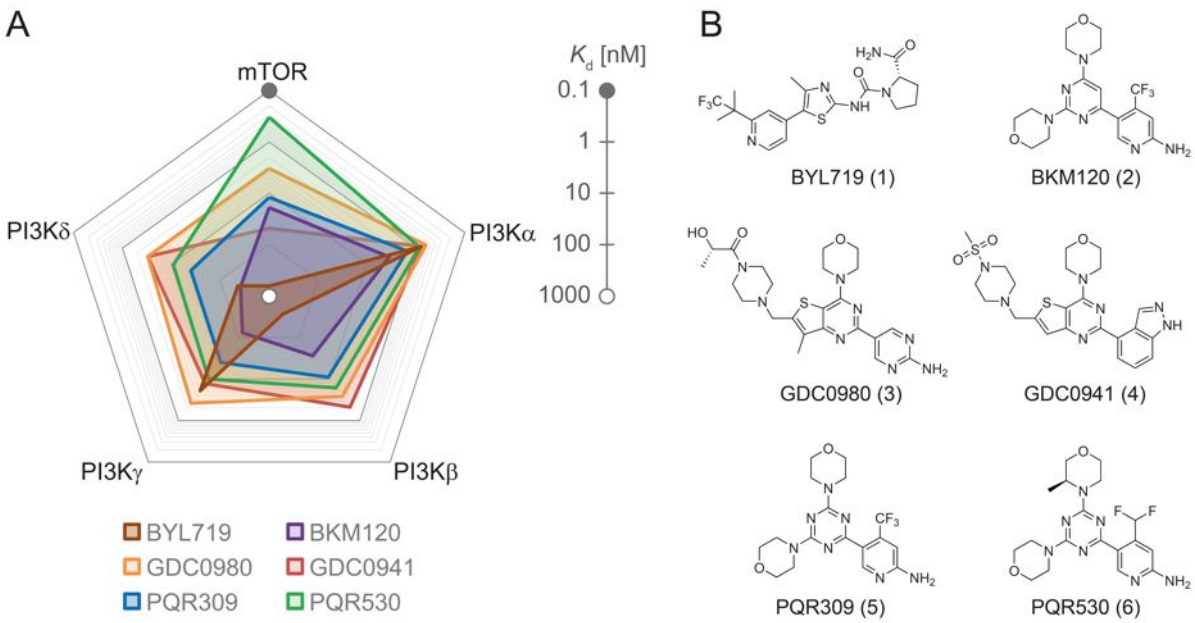

Figure 1. Affinity graph and chemical formulae of selected ATP-competitive inhibitors for class I PI3K isoforms and mTOR kinase. **A)** K_d values for each compound and kinase are presented as a radar diagram with reciprocal and logarithmic scaled axes. Data for compounds **2**, **3**, **4** and **5** are from Ref. 10. Dissociation constants (K_d) were determined using the ScanMax platform from DiscoverX,[16] see Supporting Information, Table S1. **B)** Chemical structure of clinically relevant selected compounds.

RESULTS AND DISCUSSION

Chemistry

To identify potent and dual PI3K/mTOR inhibitors with increased potency, selectivity and brain distribution profile, a library of pyrimidine and triazine compounds was produced (Scheme 1). All triazine core compounds were prepared from cyanuric chloride (**7**), either *via* di-substitution by the same morpholine moiety (M_n, route A for symmetric compounds) or by subsequent substitution with two different morpholines (route B for asymmetric compounds). Depending on the morpholine substituent, this reaction yielded the intermediates with good to excellent yields (74-87%). The heteroaryl moieties were then introduced *via* Suzuki cross-coupling using the corresponding boronic acid pinacol ester. Boronic acid pinacol esters were either protected at their 2-amino group, and isolated or generated *in situ* (see experimental section and Supporting Information). The desired triazine core derivatives (**5**, **6**, **16-22** and **31-39**) were obtained in moderate to good yields (21-87%). The synthetic procedure for the preparation of pyrimidine core compounds (**44-47**) is depicted in route C. Similar to

the synthesis of triazine derivatives, this synthesis involved a nucleophilic aromatic substitution followed by a Suzuki cross-coupling reaction. The nucleophilic aromatic substitution of 2,4,6-trichloropyrimidine by an unsubstituted morpholine to yield compounds **40** and **41** has been described previously.[9]

Scheme 1. Synthesis of tri-substituted triazine and pyrimidine core compounds.[a]

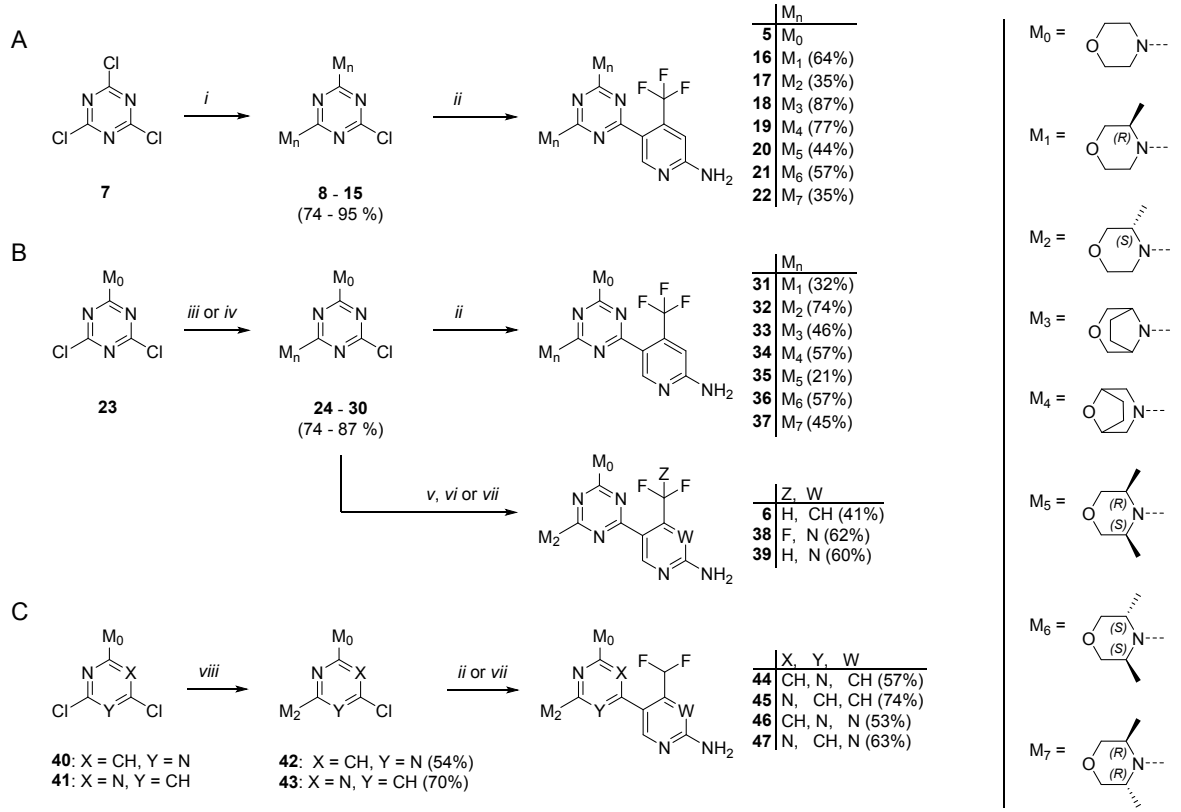

[a]Reagents and conditions: (*i*) morpholine derivative (M_n-H), CH_2Cl_2, 0 °C → rt, o/n or as reported in literature[17]; (*ii*) 1) boronic acid pinacol ester (RBpin) **48** or **49**, XPhosPdG2 (cat.), K_3PO_4, dioxane / H_2O, 95 °C, 2 - 15 h; 2) HCl, H_2O, 60 °C, 3 -15 h; (*iii*) M_n-H, DIPEA, EtOH, 0 °C → rt, o/n; (*iv*) M_n-H, DIPEA, dioxane, 70 °C, o/n; (*v*) 1) Pd(OAc) / PPh_3 (cat.), RBpin **49**, K_2CO_3, THF / H_2O, 55 °C, 2 H; 2) HCl, H_2O, 55 °C, o/n; (*vi*) RBpin, XPhosPdG2 (cat.), K_3PO_4, dioxane / H_2O, 95 °C, 2 h; (*vii*) RBpin generated *in situ* (see Supporting Information), XPhosPdG2 (cat.), K_3PO_4, dioxane / H_2O, 95 °C, 3 -15 h; (*viii*) M_n-H, DIPEA, 130 °C, o/n.

Determination of Cellular Potency and Dual PI3K and mTOR Kinase Activity

The SAR study focused initially on the exploration of substitutions on the morpholine moiety and its influence on PI3K vs. mTOR inhibition. Therefore, two series of compounds were tested (Table 1): i) symmetrical compounds (**5**, **16**-**22**), substituted with two identical morpholines ($M_{1\text{-}7}$), and ii)

asymmetric compounds (**31**-**37**), with one unsubstituted morpholine (M_0) and one substituted morpholine ($M_{1\text{-}7}$). Among the symmetric compounds, compound **20** (substituted with cis-3,5-dimethylmorpholine) had the highest affinity for both mTOR (K_i = 40 nM) and p110α (K_i = 31 nM). Overall, symmetric compounds with substituted morpholines showed increased concentrations for half-maximal inhibition (IC_{50}) of PKB/Akt and ribosomal protein S6 phosphorylation in cells. An exception was compound **17**, substituted with (*S*)-3-methylmorpholine (M_2; IC_{50} of 248 nM for pPKB and of 283 nM for pS6). With the exception of compound **31** (K_i for mTOR = 109 nM), asymmetric compounds showed a high *in vitro* potency for mTOR (K_i < 65 nM). Among this series, the most potent compounds towards PI3K and mTOR were **32** with one (*S*)-3-methylmorpholine (M_2) and **35** with cis-3,5-dimethylmorpholine (M_5; Table 1). The asymmetric compound **32** was 5-fold more potent on mTOR than its symmetric analog bearing two (*S*)-3-methylmorpholine moieties (**17**) (K_i for mTOR = 25.5 and 137 nM, respectively). Overall, compounds with only one substituted morpholine were more potently inhibiting cellular PI3K/mTOR signaling. As compound **32** showed a 2-fold increase in affinity for both PI3K and mTOR with respect to PQR309 (**5**), it was selected for further optimization.

Table 1. SAR-study of 4-(trifluoromethyl)-5-(1,3,5-triazin-2-yl)pyridine-2-amines.

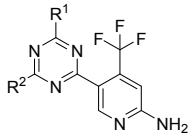

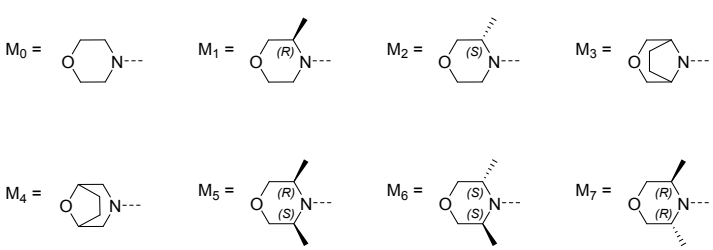

Cpd.	R^1	R^2	Cellular IC_{50}, [nM][a]		K_i, [nM][b]		K_i(p110α)/ K_i(mTOR)	clogP[c]
			pPKB	pS6	p110α	mTOR		
PQR309 (5)	M_0	M_0	139	205	17	62	0.27	3.11
16	M_1	M_1	1702	1122	684	171	4.01	3.94
17	M_2	M_2	248	283	6.8	137	0.05	3.94
18	M_3	M_3	755	299	4643	76.8	60.5	4.04
19	M_4	M_4	947	691	731	177	4.12	4.04
20	M_5	M_5	567	437	31.4	39.6	0.79	4.76
21	M_6	M_6	610	531	37.0	265	0.14	4.76
22	M_7	M_7	>20000	14522	>20000	1892	32.7	4.76
31	M_0	M_1	373	410	53.7	109	0.49	3.52
32	M_0	M_2	196	89.8	8.3	25.5	0.33	3.52
33	M_0	M_3	420	156	19.9	43.1	0.46	3.58
34	M_0	M_4	274	212	31.0	47.8	0.65	3.58
35	M_0	M_5	122	135	27.4	19.3	1.42	3.94
36	M_0	M_6	100	126	15.2	59.2	0.26	3.94
37	M_0	M_7	435	457	88.9	64.5	1.38	3.94

[a]Cellular phosphorylation of PKB/Akt on Ser473 and ribosomal S6 on Ser235/236 were analyzed in inhibitor treated A2058 melanoma cells using in-cell western detection. Each experiment performed in triplicate or as a multiple of n = 3. [b]Compounds were tested in a time-resolved FRET (TR)-assay (LanthaScreen), and inhibitor K_is were calculated for PI3Kα and mTOR as described in methods. The PI3Kα/mTOR column depicts the ratio of compound-specific PI3Kα K_i over the K_i for mTOR. Each experiment was performed at least twice or as a multiple of n = 2. [c]Marvin/JChem 16.10.17 was used for calculation of logP (partition coefficient) and PSA (polar surface area) values. For all compounds shown in this table the calculated PSA are equal to 102.5.

The results above, together with the SAR study that led to the development of a specific mTOR inhibitor, 5-[4,6-bis({3-oxa-8-azabicyclo[3.2.1]octan-8-yl})-1,3,5-triazin-2-yl]-4-(difluoromethyl)pyridin-2-amine (PQR620,[17,18] **67**; for chemical structure see Appendix S1 in

Supporting Information), encouraged the preparation of a compound series with i) a (*S*)-3-methylmorpholine and ii) a difluoro- or trifluoromethyl group on the heteroaryl moiety (Table 2). With the exception of compound **45**, both triazine (**6**, **32**, **38-39**) and pyrimidine (**44**, **46** and **47**) core compounds showed very good potencies in cells. Moreover, these data confirmed our previous observation that 4-difluoromethyl-substituted heteroaryls yielded increased affinity for mTOR, as compared to their respective 4-trifluoromethyl analogs.[17] The introduction of an additional N-atom in the heteroaryl moiety moderately improved the affinity for PI3Kα (see K_i of 1.9 nM for **39** vs. 11 nM for **6**; and K_i of 2.0 nM for **47** vs. 14 nM for **45**), but reduced mTOR binding (K_i of 192 nM for **47** vs 42 nM for **45**), allowing a fine tuning of PI3K/mTOR inhibition ratios. Although the pyrimidine core compound **44** showed a balanced PI3K/mTOR profile *in vitro*, compound **6** was selected (K_i for PI3Kα of ~ 11 nM and for mTOR of ~ 7.4 nM) for further characterization due to its superior activity in cells. Moreover, the triazine core yields symmetric compounds, and therefore eases large scale synthetic access.

Table 2. SAR of pyrimidine and triazine cores substituted with morpholine and (*S*)-3-methylmorpholine.

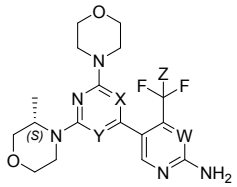

Cpd.	X	Y	Z	W	Cellular IC_{50}, [nM][a]		K_i, [nM][b]		K_i p110α/ K_i mTOR	clogP[c]	PSA[c]
					pPKB	pS6	p110α	mTOR			
32	N	N	F	CH	195.7	89.8	8.3	25.5	0.33	3.52	102.52
6	N	N	H	CH	62.2	61.9	11.1	7.4	1.50	2.80	102.52
38	N	N	F	N	91.0	164	4.0	37.9	0.11	3.08	115.41
39	N	N	H	N	32.4	63.9	1.9	10.6	0.18	2.26	115.41
44	CH	N	H	CH	146	125	11.6	10.0	1.16	2.40	89.63
45	N	CH	H	CH	614	766	13.7	42.3	0.32	2.40	89.63
46	CH	N	H	N	77.3	146	4.1	15.3	0.27	1.85	102.52
47	N	CH	H	N	99.6	387	2.0	192	0.01	1.85	102.52

[a]Cellular phosphorylation of PKB/Akt on Ser473 and ribosomal S6 on Ser235/236 were analyzed in inhibitor treated A2058 melanoma cells using in-cell western detection. Each experiment performed in triplicate or as a multiple of n = 3. [b]Compounds were tested in a time-resolved FRET (TR)-assay (LanthaScreen), and inhibitor K_is were calculated for PI3Kα and mTOR as described in methods. The PI3Kα/mTOR column depicts the ratio of compound-specific PI3Kα K_i over the K_i for mTOR. Each experiment was performed at least twice or as a multiple of n = 2. [c]Marvin/JChem 16.10.17 was used for calculation of logP (partition coefficient) and PSA (polar surface area) values.

Binding Mode to PI3K and mTOR

The binding mode and interactions of PQR309 (**5**)[10] and BKM120 (**2**)[9] with the ATP-binding site of PI3Kγ have been elucidated. In detail, the orientation of the morpholine moiety in the hinge region is well understood, and an identical binding mode for all class I PI3K isoforms can be assumed: the morpholine O-atom forms a hydrogen bond interaction with the hinge Val882 residue in PI3Kγ (Val851 in PI3Kα).

In 4-trifluoromethyl compounds with two equally substituted morpholines, morpholines M_1 (**16**), M_3 (**18**), M_4 (**19**) and M_7 (**22**) severely attenuated binding to PI3Kα (Table 1), M_5 (**20**) and M_6 (**21**) had a minor effect, while M_2 (**17**) allowed to lower the K_i for p110α to 7 nM. These results suggest that the (*S*)-enantiomer of methyl-morpholine (M_2) is well accommodated when pointing towards the hinge region (PI3Kγ: Val882, PI3Kα: Val851), while the (M_1) substitution abrogates high affinity interactions. Specifically, **17** with two (*S*)-methyl-morpholines (2x M_2) was 100-fold more potent on PI3Kα than compound **16** with two (*R*)-methyl-morpholines (2x M_1; Table 1). This tendency was reproduced by compounds with a 4-difluoromethyl substituted heteroaromatic group, where (*S*)-methyl-morpholine substitutions (for example 2x M_1 in **60**) augmented the affinity for PI3Kα by 53-fold as compared to **61** (with 2x M_2; see Table S2 in Supporting Information). The orientation of the substituted morpholines towards the hinge Val was finally confirmed with a single-sided exchange of a substituted morpholine with piperidine – thus forcing the substituted morpholine to form a H-bond with the hinge Val (compounds **63** to **65** in Table S2).

To better understand the structural basis for the different affinity between compounds with (*R*)- and (*S*)-methyl-morpholines, computational modeling studies were carried out for compound **6** and its (*R*)-enantiomer (**66**): inhibitor-PI3Kγ complexes were modelled using the PQR309 (**5**)/PI3Kγ complex crystal structure (PDB ID: 5OQ4) as a template to dock compounds with C3-substituted morpholines. As depicted in Figure 2, molecular modelling suggests a preferred placement of the (*S*)-methyl group pointing towards Tyr867 (Tyr836 in PI3Kα), while a steric clash is flagged at Ile881. The (*R*)-methyl morpholine cannot be accommodated in PI3Kγ, generating overlaps with the side chains of Ile879, Glu880 and Met953. To validate this, a compound **6**-p110α complex structure was resolved by X-ray

crystallography at a resolution of 3.15 Å (PDB ID 6OAC; Figure S1). The core structure of compound **6** could be defined in the electron density, but distinct density for the methyl groups was not apparent (Figure S1). Fitting compound **6** to the obtained electron density map, the inhibitor was best accommodated with the methyl group in one of the two hydrophobic interfaces formed by side chains of Tyr836, Ile848, Ile932 or Trp780, Ile800, and Val850 (numbering referring to PI3Kα). Val850 in PI3Kα corresponds to Ile881 in PI3Kγ, and the predicted steric clash at this position in PI3Kγ could not be detected in PI3Kα - which might explain in part a preferred binding of compound **6** to PI3Kα vs. PI3Kγ (see Table S1, K_d for PI3Kα = 0.84; K_d for PI3Kγ = 10 nM). The lack of a distinct signal for the methyl group in the X-ray structure also suggests that compound **6** can bind to PI3Ks in multiple ways, either with the substituted morpholine pointing towards the hinge region (Figure 2 and S1), or the solvent exposed space.

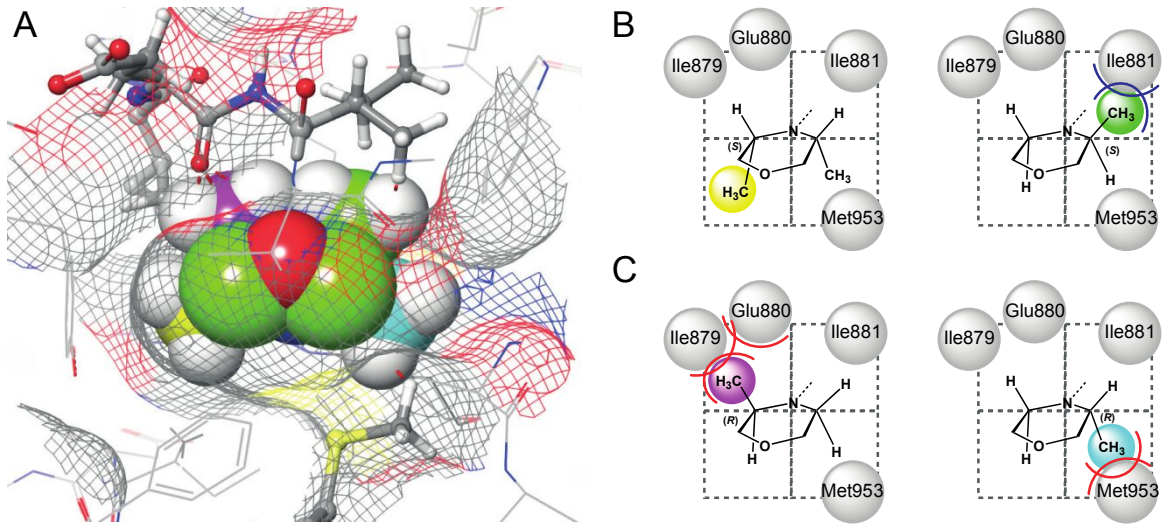

Figure 2. Model of PI3Kγ with docked compound **6** [(*S*)-enantiomer)] and its (*R*)-enantiomer **66**. **A)** The PI3Kγ surface is depicted as mesh, and selected amino acids are shown as sticks (grey). Two space filling conformations of the methyl-morpholino groups are shown for both **6** (green and yellow) and its enantiomer **66** (enantiomer, pink and cyan), oxygen atom pointing towards the hinge region Val882. The model is based on a PQR309 (**5**)-PI3Kγ complex (PDB ID: 5OQ4). Steric clashes conserved for class I PI3Ks are represented as red lines, a steric clash detected PI3Kγ is indicated in blue. **B, C)** Quadrant models for each possible position of the methyl-substituent in the hinge region of PI3Kγ are depicted for **B)** compound **6** and **C)** compound **66**. *In vitro* PI3Kα binding affinities for **6** are 11.1 nM (K_i) and 20.8 nM (K_i) for **66** (see Table S2). For the p110α-compound **6** complex see Figure S1 (deposited as PDB ID 6OAC).

A similar computational modelling analysis of the hinge region environment in mTOR showed that the ATP-binding pocket is wider: here M_1 and M_2 [(*R*)- and (*S*)-3-methylmorpholine] can be accommodated (Figure S2). These findings are supported by comparison of compound **16** to **17** (Table 1), **59** to **61** and **63** to **65** (Table S2), where mTOR affinities were very similar for M_1 and M_2 substituted compounds.

On- and Off-Target Activities

Compound **6** was selected for further elucidation of its activity profile. Binding of compound **6** to the ATP-binding site of PI3Kα was confirmed by an *in vitro* Wortmannin[19]-competition assay, where **6** prevented covalent binding of wortmannin to Lys802 in PI3Kα[20] (Figure S3). The selectivity for PI3K and mTOR over a wide range of protein and lipid kinases was validated in a KINOMEScan panel. Here, the selectivity of compound **6** was compared with data generated using the dual PI3K/mTOR inhibitor GDC0980 (**3**) and the structurally related pan-PI3K inhibitor **5**[10] (Figure S4 and Table S4). Even at 10 μM, compound **6** achieved excellent selectivity scores of S(35) = 0.052 and S(10) = 0.03, exceeding that of the dual PI3K/mTOR inhibitor **3** [S(35) = 0.22, S(10) = 0.09; exact calculation see Experimental Section; simplified: S(35): fraction of total kinases with activities reduced to <35%].

Despite these differences in *in vitro* selectivity, the sensitivities of 44 tumor cell lines to **6** and **3** showed a good overall correlation across the cell panel (Figure 3 and Table S5). Similarly, half-maximal growth inhibition (GI_{50}) of **6** (0.43 μM in a 66 tumor cell line panel) was comparable to the mean GI_{50} of 44 cell lines **3** determined earlier (GI_{50} = 0.35 μM).[9] As observed before for other PI3K/mTOR inhibitors, compound **6** acted cytostatic, and minor cytotoxicity below 10 μM was only observed in ~10% of cell lines at concentrations surpassing >>10x the GI_{50} (Table S5, individual growth curves are depicted in Figure S5).

Earlier reports have claimed that dual PI3K/mTOR inhibitors such as BEZ235[5,6,21] excel over PI3K inhibitors in the suppression of cancer cell proliferation. However, these reports usually compared inhibitors that were, however, structurally and pharmacologically very different. Indeed, the cell-specific sensitivity profile of 43 cell lines of BEZ235-mediated growth inhibition did not correlate

significantly with the well aligned profiles of **6** and **3** (Figure 3, for BEZ235 see Figure S6). A comparison of the impact of compound **6**, the structurally related PI3K inhibitor **5** and the mTOR kinase inhibitor PQR620 (**67**) on cell proliferation and PI3K/mTOR signaling confirmed an increased potency of dual PI3K/mTOR inhibition by **6** as compared to **5**, but was closely matched by **67** (Figure 4).

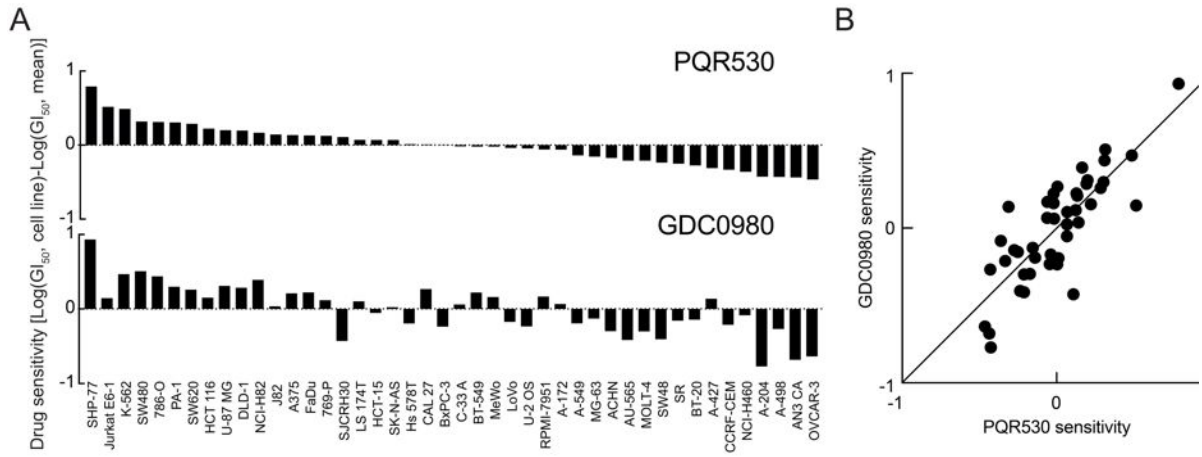

Figure 3. A) Attenuation of cell proliferation in response to PQR530 (**6**) and GDC0980 (**3**) represented as a waterfall plot. Concentrations of half-maximal growth inhibition (GI_{50}) were obtained from dose-response growth curves in 44 tumor cell lines. Log-transformed individual GI_{50} of a cell line was related to the log-transformed mean GI_{50} of all cell lines, and cell lines were sorted by lowest to highest sensitivity for PQR530 (**6**) from left to right. Individual cell lines and GI_{50}-values are given in Table S5. **B)** Correlation of **3** and **6** sensitivity of individual cell lines shown in A). The comparative dataset of **3** is from Ref. 9. Further comparisons of cellular inhibition profiles for BEZ235, compound **3**, and **5** are shown in Figures S6 and S7.

In line, compound **6** showed an increased potency in growth inhibition as compared to **5** (average over 44 cell lines: 2.5 to 3 fold lower GI_{50} and IC_{50}). The very good correlation of the cellular inhibition profiles of **5** and **6** is compatible with a similar mode of action (Figure S7).

Interestingly, half maximal growth inhibition is only achieved if phosphorylation of PKB/Akt is suppressed by ca. 90%. In SKOV3 cells, a constitutively activated p110α mutant (H1047R) drives the PI3K/mTOR pathway, while A2058 cells are devoid of the phosphoinositide 3-phosphatase PTEN, and the B-Raf V600E mutation drives the activation of the MAPK (mitogen-activated protein kinase) pathway, which contributes to an increased resistance to PI3K and mTOR inhibitors. In both tumor cell lines, increased inhibition of mTOR by **6** enhanced its ability to suppress growth proliferation over that of **5**. While **67** demonstrated similar potency in these cells, in certain oncogenic contexts a selective

TORC1 inhibitor may not be desirable due to a loss of feedback inhibition (via S6K and IRS-1) resulting in reactivation of PI3K and PKB/Akt signaling [see Ref. 17 for a comparison of rapamycin and **67**]. Thus, an inhibitor with high affinity towards both mTOR kinase and PI3K can be of advantage. The analysis of PI3K and mTOR downstream targets (PKB/Akt; GSK3β, S6K, S6) confirmed that **6** has an enhanced potential to block the pathway as compared to selective pan-PI3K or mTOR inhibitors.

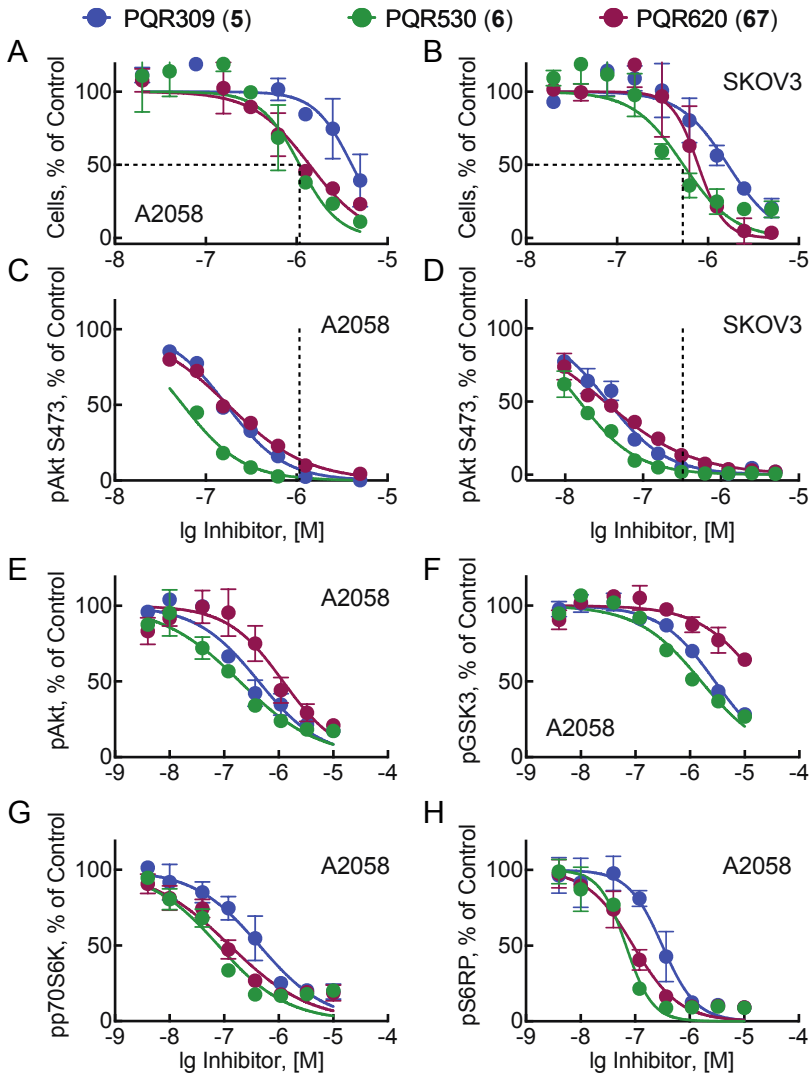

Figure 4. Impact of PI3K and mTOR inhibitors on cell proliferation and PI3K/mTOR downstream signaling. **A)** A2058 and **B)** SKOV3 cells were exposed to the indicated inhibitors for 72h; and resulting cell numbers are shown as % of DMSO controls (n = 2, mean ± SD). Dotted lines connect 50% growth inhibition with phosphorylation of PKB/Akt on Ser473, analyzed in **C)** A2058 and **D)** SKOV3 cells after exposure to the indicated inhibitors for 1h. Phosphoprotein levels were determined by an in-cell Western assay (mean ± SD, n = 3). Phosphorylation of **E)** PKB/Akt, **F)** GSK3, **G)** p70S6K and **H)** pS6 in A2058 lysates are shown as % of controls, detected using the Mesoscale Discovery platform (mean ± SD, n = 2).

Off-target effects of compound **6** were tested in a CEREP BioPrint (P22-p) panel at a concentration of 10 μM. Only very weak competitions with radioligands for cell surface and nuclear receptors, membrane channels, transporters (Table S6) and enzyme activities of kinases, proteases, and phosphodiesterases (Table S7) were detected, suggesting that **6** is a safe compound.

Pharmacological Parameters

Metabolic stability of compound **6** was assessed *in vitro* prior to *in vivo* pharmacokinetic (PK) properties. When evaluated in human, rat, dog and mouse liver microsomes, compound **6** showed little clearance after 30 minutes of exposure (Table 3A). In hepatocyte cultures, compound **6** showed low clearance in all species, dog, rat, mouse and human. The half-life of compound **6** was ~ 4.2 hours in humans and, similarly, ~ 3.2-2.6 hours in the other species (Table 3B).

Table 3A. Stability in liver microsomes of compound PQR530 (6).

	% remaining in liver microsomes[a]			
Cpd. \ species	Human	Rat	Dog	Mouse
6	81.5	106	97.4	73.2
7-EC[b]	7.45	28.5	1.8	1.5
Propranolol[b]	54.8	2.9	30.1	6.8

[a]Percentage of compound remaining after 30 minutes (mean, n=2); [b]Assay reference compounds: 7-EC, 7-Ethoxycoumarin.

Table 3B. Stability of compound PQR530 (6) in hepatocyte cultures.

Cpd. \ species		**Human**	**Rat**	**Dog**	**Mouse**
6	[a]CL_{int}	6.0	7.0	10	11
	$t_{1/2}$ [min]	250	192	142	142
7-EC[b]	CL_{int}	20.0	30	163.3	74
	$t_{1/2}$ [min]	70.0	46.2	8.49	18.7
7-HC[b]	CL_{int}	65.5	124	138	116
	$t_{1/2}$ [min]	21.1	11.1	10.2	11.9

[a]CL_{int} [µl/min/10^6 cells]; $t_{1/2}$, [min]; [b]Assay reference compounds: 7-EC, 7-Ethoxycoumarin; 7-HC, 7-Hydroxycoumarin; Results are expressed as mean, n=3.

Subsequently, PK parameters of compound **6** were assessed in male C57BL/6J mice using a single oral dose of 50 mg/kg (Table 4 and Figure 5). Drug levels were determined by LC-MS/MS in extracts of plasma, brain and thigh muscle. Half-life was determined to be approximately 3.5 - 4.8 hours. Concentration of compound **6** in the brain was higher than in plasma (C_{max} of ~ 7799 ng/mL in plasma

and of ~ 12627 ng/mL in brain), demonstrating that compound **6** passes the blood-brain barrier, showing a ca. 1:1.67 distribution between plasma and brain. The maximal concentration was reached after 30 minutes in plasma, brain and thigh muscles.

The observed brain/plasma ratio corresponded with parallel artificial membrane permeability assay (PAMPA, Table S8A) and MDCK permeability assays, which documented a fast and passive diffusion. The lack of effect of the addition of the P-glycoprotein P-gp (P-glycoprotein 1, MDR1) inhibitor cyclosporine A to the MDCK assay demonstrates, that **6** is not a substrate for P-gp transport (see Table S8B), which predicts excellent brain penetration. Finally, a brain tissue binding assay revealed a fu (fraction unbound) value of ~8%, which closely matched the levels of diazepam (fu ~9%, Table S8C) with a proven brain activity. Altogether, the assembled parameters characterize **6** as a compound with high on-target potency in brain tissue.

Table 4. PK analysis of PQR530 (6) after oral application in male C57BL/6J mice (50 mg/kg p.o.).

	Plasma	**Brain**	**Thigh muscle**
C_{max} [ng/mL]	7799	12627	11946
T_{max} [h]	0.5	0.5	0.5
$t_{1/2}$ [h]	4.7	4.8	3.5
AUC_{0-8h} [h*ng/mL]	27910	46483	39248
Cl [mL/h/kg]	1257	729	1003

p.o.: per os; C_{max}: maximal concentration, T_{max}: time of maximal concentration in hours; $t_{1/2}$: half-life elimination in hours; AUC: area under the curve, Cl: clearance; (n=3, mean for each time-point).

The physiological effect of compound **6** administration on plasma glucose and insulin levels in male C57BL/6J mice is shown in Figure 5: vehicle treatment did not affect plasma insulin or glucose levels, while compound **6** triggered an increase in plasma glucose and insulin levels. Ten minutes after treatment with compound **6**, plasma glucose levels rose significantly as compared to vehicle, and reached maximal concentrations one hour after dosing. Plasma insulin levels reached maxima two hours post-dosing. The rise of plasma glucose and insulin levels are typical for PI3K/mTOR pathway inhibitors[22] and have also been observed with pan-PI3K inhibitors, such as **5**, in preclinical[10] and phase I clinical studies.[15]

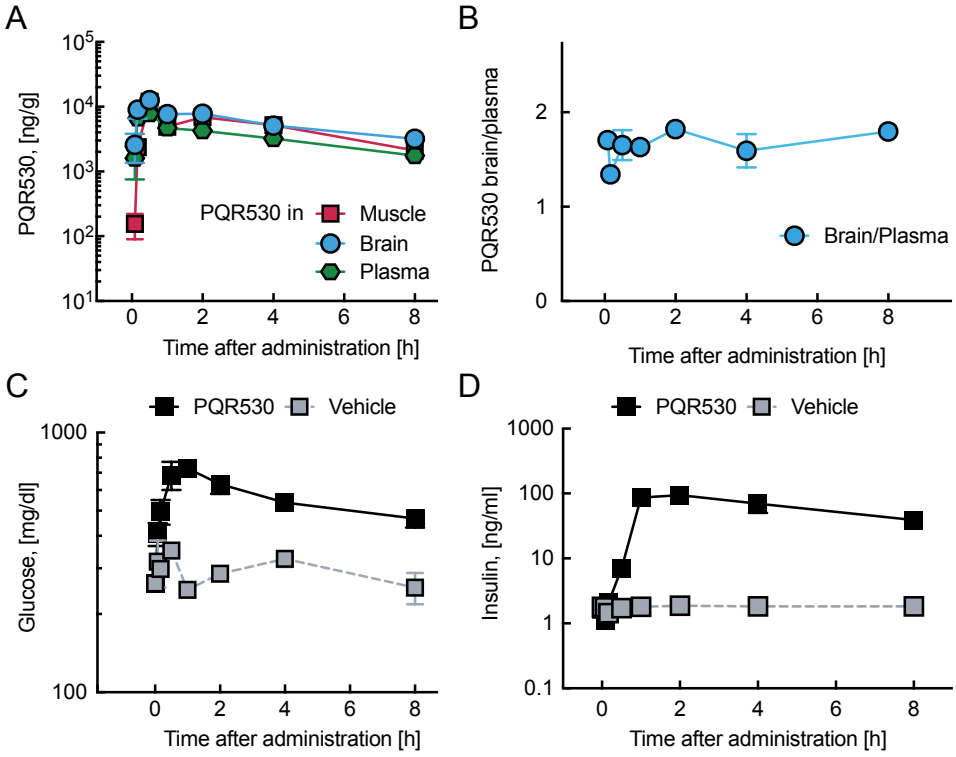

Figure 5. PK/PD assessment of PQR530 (**6**) *in vivo*. Compound **6** was administered to male C57BL/6J mice as single dose per os (p.o., 50 mg/kg). **A)** Levels of **6** in C57BL/6J mouse tissues (n=3). Compound **6** was extracted from each tissue at the indicated time-points, and was subsequently quantified using LC-MS. **B)** Tissue distribution ratios of **6**. Data of **6** in (B) was compared to rapamycin and everolimus in Ref. 18. **C)** Glucose concentration after oral application in male C57BL/6J mice. Plasma glucose was quantified using the Glucose Calorimetric Assay Kit (cat. No. Cay10009582-192, Biomol, Germany). **D)** Plasma insulin levels in male C57BL/6J mice were quantified using a commercially available colorimetric immunoassay kit (Rat/Mouse Insulin ELISA, cat. No. EZRMI-13K, Merck Millipore, Germany). All values mean ± SEM. Error bars not shown when smaller than the symbols. A comparison of PK and brain/plasma distribution values of **6** with PQR309 (**5**) is shown in Figure S8.

In vitro and *in vivo* toxicokinetic parameters were determined in rats and dogs and are summarized in Table S9. The side effects of compound **6** were consistent with its mechanism of action. In Wistar rats, the no-observed adverse effect level (NOAEL) of compound **6** was considered to be 1 mg/kg/day for males and 0.5 mg/kg for females (corresponding to steady state $AUC_{0\text{-}8}$ levels of 335 h·ng/mL and 599 h·ng/mL, respectively). In Beagle dogs, the no-observed adverse effect level (NOAEL) of compound **6** was 1 mg/kg/day for males (corresponding to steady state AUC_{last} levels of 127 ± 45 h·ng/mL) and 3 mg/kg/day for females (corresponding to steady state AUC_{last} levels of 1070 ± 596 h·ng/mL).

In vivo Efficacy of PQR530 (6)

In order to establish the antiproliferative effect of compound **6** *in vivo*, an OVCAR-3 xenograft model in BALB/c nude mice was used (Figure 6). To initiate tumor development, mice were inoculated subcutaneously (region of right flank) with OVCAR-3 cells at day 0. From day 17, the control group received vehicle once a day (QD), while the treated group received 25 mg/kg of compound **6** p.o. QD. Compared to vehicle treated mice, compound **6** significantly inhibited tumor growth. No significant body weight loss was observed.

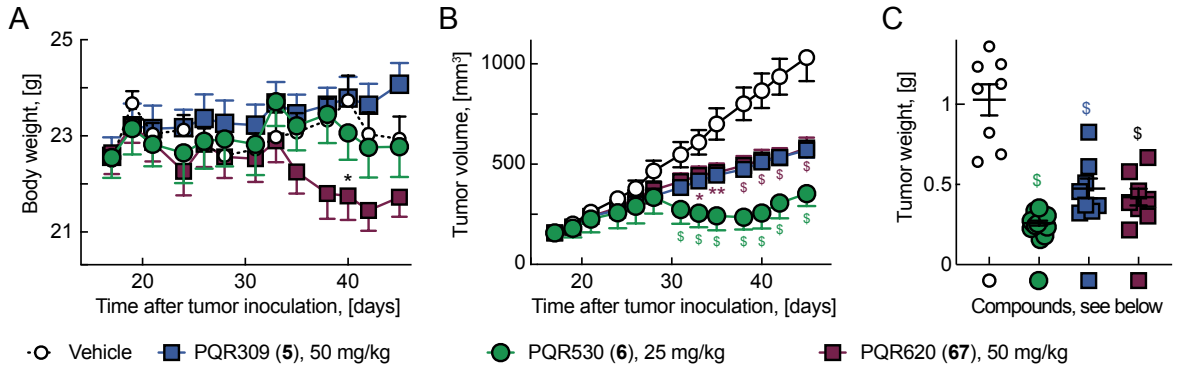

Figure 6. OVCAR-3 human ovarian cancer xenograft model in BALB/c nude mice: tumor cells were subcutaneously inoculated at day 0, and daily oral application of the indicated agents was started at day 17 (28 x QD). **A)** body weight was determined at the depicted time points. **B)** The tumor size was measured and calculated as described in the experimental section. **C)** The tumor weight was determined at day 45. Statistics: (*p<0.05; **p<0.001; $p<0.0001; n=8; (A,B) Two-Way ANOVA with Bonferroni or Dunnett's correction for multi-comparisons, mean ± SEM; (C) mean ± SEM; One-Way ANOVA with Tukey's correction for multi-comparisons. PQR620 (**67**) and vehicle data were shown in Ref. 17.

CONCLUSION

An extensive SAR study led to the identification of **6**, a potent ATP competitive dual pan-PI3K and mTORC1/2 inhibitor with a sub-nanomolar K_d towards PI3Kα and mTOR (0.84 and 0.33 nM, respectively). Compound **6** shows improved potency against mTOR kinase as compared to other advanced candidates with dual pan-class I PI3K and mTOR inhibitory activity. Molecular modeling and X-ray crystallography elucidated interactions of **6** in the ATP-binding pocket of PI3Ks and mTOR. The selectivity of **6** for PI3Ks and mTOR over a wide range of protein and lipid kinases, a lack of detectable off-target effects, *in vitro* and *in vivo* toxicity studies highlight the safety of **6**. Compound **6**

displayed potency in inhibiting cancer cell line proliferation, and pharmacokinetic studies of **6** showed good bioavailability and excellent brain penetration, culminating in a good *in vivo* efficacy in an OVCAR-3 xenograft model. Altogether, the present results encourage the further development of the compound as a clinical candidate in oncology.

EXPERIMENTAL SECTION

General Information

Reagents were purchased at the highest commercial quality from Acros, Sigma-Aldrich or Fluorochem and used without further purification. Solvents were purchased from Acros Organics in AcroSeal® bottles over molecular sieves. Cross coupling reactions were carried out under nitrogen atmosphere in anhydrous solvents, and glassware was oven dried prior to use. Thin layer chromatography (TLC) plates were purchased from Merck KGaA (Polygram SIL / UV254, 0.2 mm silica with fluorescence indicator) and UV light (254 nm) was used to visualize the compounds. Column chromatographic purifications were performed on Merck KGaA silica gel (pore size 60 Å, 230-400 mesh particle size). Alternatively, flash chromatography was performed with Isco CombiFlash Companion systems using prepacked silica gel columns (40 - 60 μm particle size RediSep). ^{1}H, ^{19}F and ^{13}C NMR spectra were recorded on a Bruker Avance 400 spectrometer. NMR spectra were obtained in deuterated solvents, such as $CDCl_3$ or $(CD_3)_2SO$. The chemical shift (δ values) are reported in ppm and corrected to the signal of the deuterated solvents (7.26 ppm (^{1}H NMR) and 77.16 ppm (^{13}C NMR) for $CDCl_3$; and 2.50 ppm (^{1}H NMR) and 39.52 ppm (^{13}C NMR) for $(CD_3)_2SO$. ^{19}F NMR spectra are calibrated relative to $CFCl_3$ (δ = 0 ppm) as external standard. When peak multiplicities are reported, the following abbreviations are used: s (singlet), d (doublet), dd (doublet of doublets), t (triplet), td (triplet of doublets), q (quartet), m (multiplet), br (broadened). Coupling constants, when given, are reported in Hertz (Hz). High resolution mass spectra (HRMS) were recorded on a Thermo Fisher Scientific LTQ Orbitrap XL (nanoESI-MS) spectrometer. MALDI-ToF mass spectra were obtained on a Voyager-De™ Pro measured in *m/z*. The chromatographic purity of final compounds was determined by high performance liquid chromatography (HPLC) analyses on an Ultimate 3000SD System from ThermoFisher with LPG-3400SD pump system, ACC-3000 autosampler and column oven, and DAD-3000 diode array detector. An Acclaim-120 C18 reversed-phase column from ThermoFisher was used as stationary phase. Gradient elution (5:95 for 0.2 min, 5:95 → 100:0 over 10 min, 100:0 for 3 min) of the mobile phase consisting of CH_3CN / MeOH:$H_2O_{(10:90)}$ was used at a flow rate of 0.5 mL / min at 40 °C. The purity of all final compounds was higher than 95%.

General procedure 1.

Step 1. Monochloro-triazine or -pyrimidine derivative (1.0 equiv), boronic acid pinacol ester **48** or **49** (1.0 - 1.1 equiv), K_3PO_4 (2.0-3.0 equiv) and chloro(2-dicyclohexylphosphino-2′,4′,6′-triisopropyl-1,1′-biphenyl)[2-(2′-amino-1,1′-biphenyl)]palladium(II) (XPhos Pd G2, 0.05 equiv) were charged in a flask. Under nitrogen atmosphere, absolute 1,4-dioxane (approx. 1 mL / 0.2 mmol) and deionized H_2O (approx. 1 mL / 0.4 mmol) were added and the resulting mixture was placed into an oil bath pre-heated at 95 °C and stirred at this temperature for 3-15 hours. After completion of the reaction, the mixture was allowed to cool down to room temperature. *Step 2.* A 3 M aqueous HCl-solution (> 10 equiv) was added and the resulting mixture was heated at 60 °C for 3-15 hours. Reaction completion was monitored by TLC. The mixture was allowed to cool down to room temperature, the pH was adjusted to 8-9 by addition of a 2 M aqueous NaOH-solution and the aqueous layer was extracted with ethyl acetate (3 x). The combined organic layers were dried over anhydrous Na_2SO_4, filtered and the solvent was evaporated under reduced pressure. The crude product was purified by column chromatography on silica gel.

General procedure 2.

To a solution of 4-(4,6-dichloro-1,3,5-triazin-2-yl)morpholine (**23**, 1.0 equiv) in 1,4-dioxane (approx. 1 mL / 0.3 mmol), the respective morpholine derivative (1.0 - 1.2 equiv) and *N*,*N*-diisopropylethylamine (4.5 - 4.7 equiv) were added. The resulting mixture was stirred at 70 °C overnight. The solvent was then removed under reduced pressure and the residue was purified by column chromatography on silica gel.

General procedure 3.

Step 1. Bis(pinacolato)diboron (1.5 equiv), potassium acetate (3.0 equiv), [1,1′-bis(diphenylphosphino)ferrocene]dichloropalladium(II) ($Pd(dppf)Cl_2$, 0.10 equiv) and the respective bromo derivative (1.0 equiv) were dissolved in absolute 1,4-dioxane (approx. 1 mL / 0.2 mmol) under nitrogen atmosphere. The resulting mixture was heated at 95 °C for 6-8 hours. *Step 2.* Then, the mixture was allowed to cool down to room temperature. Monochloro-triazine or -pyrimidine derivative (1.1

equiv), chloro(2-dicyclohexylphosphino-2′,4′,6′-triisopropyl-1,1′-biphenyl)[2-(2′-amino-1,1′-biphenyl)]palladium(II) (XPhos Pd G2, 0.05 equiv), K_3PO_4 (2.0 equiv) and deionized H_2O (approx. 1 mL / 0.4 mmol) were added. The resulting reaction mixture was placed in a preheated oil bath at 95 °C and stirred for 3-15 hours. After completion of the reaction, the mixture was allowed to cool down to room temperature, deionized H_2O was added and the mixture was extracted with dichloromethane (3 x). The combined organic layers were washed with brine (2 x), dried over anhydrous Na_2SO_4, filtered and reduced to dryness under reduced pressure. *Step 3.* The above residue was dissolved in 1,4-dioxane (approx. 1 mL / 0.1 mmol) and an aqueous solution of HCl (3 M, 10-15 equiv) was added. The reaction mixture was stirred at 60 °C for 2 hours. The mixture was diluted with deionized H_2O and washed with ethyl acetate (1 x). The aqueous layer was basified to pH = 10 and then extracted with ethyl acetate (3 x). The combined organic layers were dried over anhydrous Na_2SO_4, filtered and reduced to dryness under reduced pressure. The crude product was purified by column chromatography on silica gel.

General procedure 4.

To a solution of the desired dichloropyrimidine (**40** or **41**, 1.0 equiv) in *N*,*N*-dimethylformamide (approx. 1 mL / 0.3 mmol), the respective morpholine derivative (1.5 equiv) and *N*,*N*-diisopropylethylamine (3.0 equiv) were added. The resulting mixture was stirred at 130°C overnight. The solvent was then removed under reduced pressure and the residue was dissolved in dichloromethane. The organic layer was washed with aqueous saturated $NaHSO_4$-solution, dried over anhydrous Na_2SO_4, filtered and the solvent was evaporated under reduced pressure. The crude product was purified by column chromatography on silica gel.

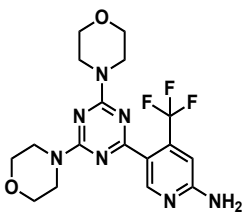

5-[4,6-Bis(morpholin-4-yl)-1,3,5-triazin-2-yl]-4-(trifluoromethyl)pyridin-2-amine (**PQR309**, **5**). Compound **5** was prepared according to the literature.[9]

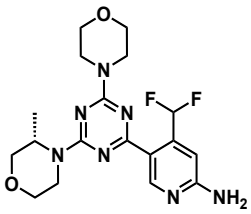

4-(Difluoromethyl)-5-{4-[(3*S*)-3-methylmorpholin-4-yl]-6-(morpholin-4-yl)-1,3,5-triazin-2-yl}pyridin-2-amine (PQR530, 6). $Pd(OAc)_2$ (538 mg, 2.40 mmol, 0.04 equiv) and PPh_3 (1.89 g, 7.21 mmol, 0.12 equiv) were dissolved in tetrahydrofuran (50 mL) and stirred at room temperature for 1 hour. This solution was added to a mixture of boronic acid pinacol ester **49** (19.5 g, 60.0 mmol, 1.0 equiv), intermediate **25** (18.0 g, 60.0 mmol, 1.0 equiv) and aqueous K_2CO_3 (2.4 M, 81.0 mL, 194 mmol, 3.2 equiv) in tetrahydrofuran (200 mL). Then, the reaction mixture was heated at 55 °C for 2 hours. After this time, the reaction mixture was allowed to cool down to room temperature and an aqueous HCl-solution (5 M, 123 mL, 615 mmol, 10 equiv) was slowly added. The resulting reaction mixture was heated at 55 °C overnight. Upon completion of the reaction, the mixture was allowed to cool down to room temperature and tetrahydrofuran was removed under reduced pressure. The pH was adjusted to 9 by addition of NaOH pellets. The aqueous layer was extracted with 2-methyltetrahydrofuran (2 x 200 mL). The combined organic layers were dried over anhydrous Na_2SO_4, filtered and concentrated to dryness under reduced pressure. The residue was purified by column chromatography on silica gel (cyclohexane / ethyl acetate 1:0 → 7:3) to afford compound **6** as a colorless solid (10.2 g, 25.0 mmol, 41%). **^{1}H NMR** (400 MHz, $CDCl_3$): δ 9.03 (s, 1 H), 7.67 (t, $^1J_{H,F}$ = 55 Hz, 1 H), 6.84 (s, 1 H), 4.84 (br s, 2 H), 4.78-4.69 (m, 1 H), 4.45-4.34 (m, 1 H), 3.97 (dd, $J_{H,H}$ = 11, 3.7 Hz, 1 H), 3.89-3.71 (m, 9 H), 3.68 (dd, $J_{H,H}$ = 12, 3.2 Hz, 1 H), 3.52 (td, $J_{H,H}$ = 12, 3.0 Hz, 1 H), 3.27 (td, $J_{H,H}$ = 13, 3.8 Hz, 1 H), 1.32 (d, $^3J_{H,H}$ = 6.8 Hz, 3 H). **^{19}F{^{1}H} NMR** (376 MHz, $CDCl_3$): δ − 115.9 (s, 2 F). **^{13}C{^{1}H} NMR** (101 MHz, $CDCl_3$): δ 169.4 (s, 1 C), 164.9 (s, 1 C), 164.5 (s, 1 C), 160.2 (s, 1 C), 152.5 (s, 1 C), 143.7 (t, $^2J_{C,F}$ = 22 Hz, 1 C), 121.6 (t, $^3J_{C,F}$ = 4.6 Hz, 1 C), 111.5 (t, $^1J_{C,F}$ = 239 Hz, 1 C), 104.1 (t, $^3J_{C,F}$ = 7.9 Hz, 1 C), 71.2 (s, 1 C), 67.1 (s, 1 C), 66.9 (br s, 2 C), 46.5 (s, 1 C), 43.8 (br s, 2 C), 38.7 (s, 1 C), 14.4 (s, 1 C). **NSI-HRMS** (*m/z*): $[M + H]^+$ calc. for $C_{18}H_{24}F_2N_7O_2$, 408.1954; found: 408.1940. **HPLC**: t_R = 7.73 min (99.1% purity).

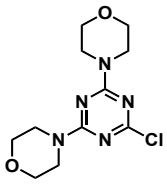

2-Chloro-4,6-bis(morpholin-4-yl)-1,3,5-triazine (8). Compound **8** was prepared according to the literature.[9]

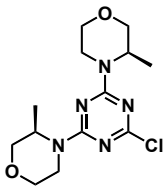

2-Chloro-4,6-bis[(3*R*)-3-methylmorpholin-4-yl]-1,3,5-triazine (9). Compound **9** was prepared according to the literature.[17]

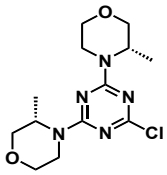

2-Chloro-4,6-bis[(3*S*)-3-methylmorpholin-4-yl]-1,3,5-triazine (10). To a solution of cyanuric chloride (868 mg, 4.70 mmol, 1.0 equiv) in dichloromethane (20 mL) at 0 °C, a solution of (*S*)-3-methylmorpholine (2.00 g, 19.8 mmol, 4.2 equiv) in dichloromethane (20 mL) was slowly added. The resulting reaction mixture was stirred overnight, while it was allowed to warm up to room temperature. Additional dichloromethane (50 mL) was added and the organic layer was washed with an aqueous saturated $NaHSO_4$-solution (2 x). The organic layer was dried over anhydrous Na_2SO_4, filtered and the solvent was evaporated under reduced pressure. The crude product was purified by column chromatography on silica gel (cyclohexane / ethyl acetate 1:0 → 3:1) to afford compound **10** as a colorless solid (1.40 g, 4.46 mmol, 95%). **^{1}H NMR** (400 MHz, $CDCl_3$): δ 4.76-4.53 (m, 2 H), 4.39-4.22 (m, 2 H), 3.93 (dd, $J_{H,H}$ = 11, 3.7 Hz, 2 H), 3.72 (d, $J_{H,H}$ = 11 Hz, 2 H), 3.63 (dd, $J_{H,H}$ = 11, 3.2 Hz, 2 H), 3.48 (td, $J_{H,H}$ = 12, 3.0 Hz, 2 H), 3.29-3.19 (m, 2 H), 1.30 (d, $^3J_{H,H}$ = 6.9 Hz, 6 H). **^{13}C{^{1}H} NMR**

(101 MHz, $CDCl_3$): δ 169.7 (s, 1 C), 164.3 (s, 2 C), 71.0 (s, 2 C), 67.0 (s, 2 C), 46.8 (s, 2 C), 38.9 (s, 2 C), 14.6 (br s, 2 C). **MALDI-MS**: *m/z* = 314.4 ($[M + H]^+$).

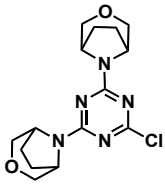

8-(4-Chloro-6-{3-oxa-8-azabicyclo[3.2.1]octan-8-yl}-1,3,5-triazin-2-yl)-3-oxa-8-azabicyclo[3.2.1]octane (**11**). Compound **11** was prepared according to the literature.[9]

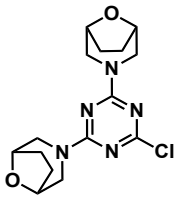

3-(4-Chloro-6-{8-oxa-3-azabicyclo[3.2.1]octan-3-yl}-1,3,5-triazin-2-yl)-8-oxa-3-azabicyclo[3.2.1]octane (**12**). Compound **12** was prepared according to the literature.[17]

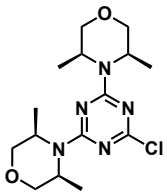

2-Chloro-4,6-bis[(3*R*,5*S*)-3,5-dimethylmorpholin-4-yl]-1,3,5-triazine (**13**). Compound **13** was prepared according to the literature.[17]

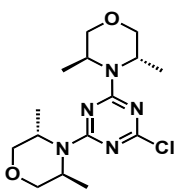

2-Chloro-4,6-bis[(3*S*,5*S*)-3,5-dimethylmorpholin-4-yl]-1,3,5-triazine (**14**). Compound **14** was prepared according to the literature.[17]

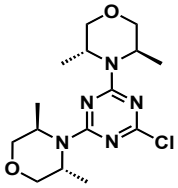

2-Chloro-4,6-bis[(3*R*,5*R*)-3,5-dimethylmorpholin-4-yl]-1,3,5-triazine (**15**). Compound **15** was prepared according to the literature.[17]

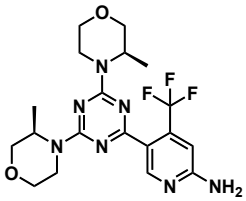

5-{4,6-Bis[(3*R*)-3-methylmorpholin-4-yl]-1,3,5-triazin-2-yl}-4-(trifluoromethyl)pyridin-2-amine (16). Compound **16** was prepared according to general procedure 1 from intermediate **9** (80.0 mg, 255 µmol, 1.0 equiv) and boronic acid pinacol ester **48** (87.1 mg, 254 µmol, 1.0 equiv). Purification by column chromatography on silica gel (cyclohexane / ethyl acetate 1:0 →4:6) gave compound **16** as a colorless solid (71.0 mg, 162 µmol, 64%). **^{1}H NMR** (400 MHz, $CDCl_3$): δ 8.72 (s, 1 H), 6.78 (s, 1 H), 4.91 (br s, 2 H), 4.85-4.70 (m, 2 H), 4.51-4.33 (m, 2 H), 3.95 (dd, $^2J_{H,H}$ = 11 Hz, $^3J_{H,H}$ = 3.6 Hz, 2 H), 3.74 (d, $^2J_{H,H}$ = 11 Hz, 2 H), 3.66 (dd, $^2J_{H,H}$ = 11 Hz, $^3J_{H,H}$ = 3.2 Hz, 2 H), 3.51 (td, $J_{H,H}$ = 12, 3.0 Hz, 2 H), 3.31-3.19 (m, 2 H), 1.32 (d, $^3J_{H,H}$ = 6.8 Hz, 6 H). **^{19}F{^{1}H} NMR** (376 MHz, $CDCl_3$): δ − 60.2 (s, 3 F). **^{13}C{^{1}H} NMR** (101 MHz, $CDCl_3$): δ 169.9 (s, 1 C), 164.5 (s, 2 C), 159.6 (s, 1 C), 152.9 (s, 1 C), 138.5 (q, $^2J_{C,F}$ = 33 Hz, 1 C), 123.0 (q, $^1J_{C,F}$ = 274 Hz, 1 C), 122.6 (s, 1 C), 105.7-105.2 (s, 1 C), 71.2 (s, 2 C), 67.2 (s, 2 C), 46.4 (s, 2 C), 38.6 (s, 2 C), 14.4 (s, 2 C). **NSI-HRMS** (*m/z*): $[M + H]^+$ calc. for $C_{19}H_{25}F_3N_7O_2$, 440.2016; found: 440.2007. **HPLC**: t_R = 8.50 min (98.1% purity).

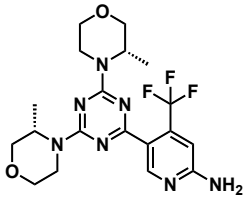

5-{4,6-Bis[(3*S*)-3-methylmorpholin-4-yl]-1,3,5-triazin-2-yl}-4-(trifluoromethyl)pyridin-2-amine (17). Compound **17** was prepared according to general procedure 1 from intermediate **10** (700 mg, 2.23 mmol, 1.0 equiv) and boronic acid pinacol ester **48** (770 mg, 2.24 mmol, 1.0 equiv). Purification by column chromatography on silica gel (cyclohexane / ethyl acetate 1:2 → 1:3) gave compound **17** as a colorless solid (344 mg, 782 µmol, 35%). **^{1}H NMR** (400 MHz, $CDCl_3$): δ 8.70 (s, 1 H), 6.76 (s, 1 H), 4.84 (br s, 2 H), 4.81-4.69 (m, 2 H), 4.48-4.30 (m, 2 H), 3.93 (dd, $^2J_{H,H}$ = 11 Hz, $^3J_{H,H}$ = 3.7 Hz, 2 H), 3.73 (d, $^2J_{H,H}$ = 11 Hz, 2 H), 3.64 (dd, $^3J_{H,H}$ = 12 Hz, $^2J_{H,H}$ = 3.2 Hz, 2 H), 3.55-3.45 (m, 2 H), 3.28-3.18 (m, 2 H), 1.30 (d, $^3J_{H,H}$ = 6.8 Hz, 6 H). **^{19}F{^{1}H} NMR** (376 MHz, $CDCl_3$): δ − 60.2 (s, 3 F). **^{13}C{^{1}H} NMR** (101 MHz, $CDCl_3$): δ 169.9 (s, 1 C), 164.5 (s, 2 C), 159.6 (s, 1 C), 152.8 (s, 1 C), 138.5 (q, $^2J_{C,F}$ = 33 Hz, 1 C), 123.0 (q, $^1J_{C,F}$ = 274 Hz, 1 C), 122.5 (s, 1 C), 105.7-105.1 (s, 1 C), 71.2 (s, 2 C), 67.1 (s, 2 C), 46.4 (s, 2 C), 38.5 (s, 2 C), 14.4 (s, 2 C). **NSI-HRMS** (*m/z*): $[M + H]^+$ calc. for $C_{19}H_{25}F_3N_7O_2$, 440.2016; found: 440.2006. **HPLC**: t_R = 8.49 min (99.0% purity).

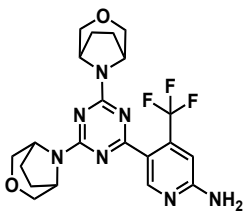

5-[4,6-Bis({3-oxa-8-azabicyclo[3.2.1]octan-8-yl})-1,3,5-triazin-2-yl]-4-(trifluoromethyl)pyridin-2-amine (18). Compound **18** was prepared according to general procedure 1 from intermediate **11** (100 mg, 296 µmol, 1.0 equiv) and boronic acid pinacol ester **48** (112 mg, 325 µmol, 1.1 equiv). Purification by column chromatography on silica gel (cyclohexane / ethyl acetate 1:0 → 3:7) gave compound **18** as a colorless solid (118 mg, 255 µmol, 87%). **^{1}H NMR** (400 MHz, $CDCl_3$): δ 8.71 (s, 1 H), 6.77 (s, 1H), 4.90 (br s, 2 H), 4.80-4.59 (m, 4 H), 3.83-3.73 (m, 4 H), 3.67-3.58 (m, 4

H), 2.13-1.92 (m, 8 H). **^{19}F{^{1}H} NMR** (376 MHz, $CDCl_3$): δ − 59.9 (s, 3 F). **^{13}C{^{1}H} NMR** (101 MHz, $CDCl_3$): δ 170.4 (s, 1 C), 163.4 (s, 2 C), 159.6 (s, 1 C), 152.8 (s, 1 C), 138.5 (q, $^{2}J_{C,F}$ = 33 Hz, 1 C), 123.0 (q, $^{1}J_{C,F}$ = 274 Hz, 1 C), 122.5 (s, 1 C), 105.5 (q, $^{3}J_{C,F}$ = 6.0 Hz, 1 C), 72.1 (s, 2 C), 71.7 (s, 2 C), 54.9 (s, 2 C), 54.5 (s, 2 C), 27.0 (s, 4 C). **NSI-HRMS** (*m/z*): $[M + H]^+$ calc. for $C_{21}H_{25}F_3N_7O_2$, 464.2016; found: 464.1999. **HPLC**: t_R = 8.33 min (97.1% purity).

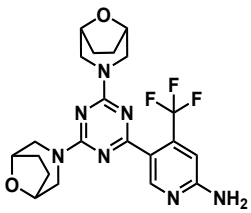

5-[4,6-Bis({8-oxa-3-azabicyclo[3.2.1]octan-3-yl})-1,3,5-triazin-2-yl]-4-(trifluoromethyl)pyridin-2-amine (19). Compound **19** was prepared according to general procedure 1 from intermediate **12** (100 mg, 296 µmol, 1.0 equiv) and boronic acid pinacol ester **48** (112 mg, 325 µmol, 1.1 equiv). Purification by column chromatography on silica gel (cyclohexane / ethyl acetate 1:0 → 3:7) gave compound **19** as a colorless solid (105 mg, 227 µmol, 77%). **^{1}H NMR** (400 MHz, $CDCl_3$): δ 8.69 (s, 1 H), 6.77 (s, 1 H), 4.89 (br s, 2 H), 4.48-4.37 (m, 6 H), 4.35-4.25 (m, 2 H), 3.21-3.12 (m, 4 H), 1.97-1.87 (m, 4 H), 1.83-1.73 (m, 4 H). **^{19}F{^{1}H} NMR** (376 MHz, $CDCl_3$): δ − 59.8 (s, 3 F). **^{13}C{^{1}H} NMR** (101 MHz, $CDCl_3$): δ 169.6 (s, 1 C), 165.7 (s, 2 C), 159.6 (s, 1 C), 152.8 (s, 1 C), 138.5 (q, $^{2}J_{C,F}$ = 33 Hz, 1 C), 123.0 (q, $^{1}J_{C,F}$ = 274 Hz, 1 C), 122.7 (s, 1 C), 105.4 (q, $^{3}J_{C,F}$ = 5.7 Hz, 1 C), 74.2 (s, 2 C), 74.0 (s, 2 C), 49.4 (s, 2 C), 49.1 (s, 2 C), 27.9 (s, 2 C), 27.7 (s, 2 C). **NSI-HRMS** (*m/z*): $[M + H]^+$ calc. for $C_{21}H_{25}F_3N_7O_2$, 464.2016; found: 464.1998. **HPLC**: t_R = 8.07 min (97.1% purity).

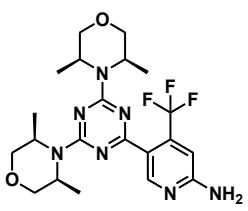

5-{4,6-Bis[(3*R*,5*S*)-3,5-dimethylmorpholin-4-yl]-1,3,5-triazin-2-yl}-4-(trifluoromethyl)pyridin-2-amine (20). Compound **20** was prepared according to general procedure 1 from intermediate **13** (48.0

mg, 140 µmol, 1.0 equiv) and boronic acid pinacol ester **48** (53.0 mg, 154 µmol, 1.1 equiv). Purification by column chromatography on silica gel (cyclohexane / ethyl acetate 1:0 → 1:1) gave compound **20** as a colorless solid (29.3 mg, 62.7 µmol, 44%). **^{1}H NMR** (400 MHz, $CDCl_3$): δ 8.78 (s, 1 H), 6.79 (s, 1 H), 4.82 (br s, 2 H), 4.71-4.50 (m, 4 H 3.82 (d, $^2J_{H,H}$ = 11 Hz, 4 H), 3.64 (dd, $^2J_{H,H}$ = 11 Hz, $^3J_{H,H}$ = 3.4 Hz, 4 H), 1.37 (d, $^3J_{H,H}$ = 6.9 Hz, 12 H). **^{19}F{^{1}H} NMR** (376 MHz, $CDCl_3$): δ − 60.4 (s, 3 F). **^{13}C{^{1}H} NMR** (101 MHz, $CDCl_3$): δ 169.6 (s, 1 C), 164.2 (s, 2 C), 159.4 (s, 1 C), 153.1 (s, 1 C), 138.5 (q, $^2J_{C,F}$ = 33 Hz, 1 C), 123.0 (q, $^1J_{C,F}$ = 274 Hz, 1 C), 122.9 (s, 1 C), 105.4 (q, $^3J_{C,F}$ = 5.7 Hz, 1 C), 71.6 (s, 4 C), 45.7 (s, 4 C), 19.3 (br s, 4 C). **NSI-HRMS** (*m/z*): $[M + H]^+$ calc. for $C_{21}H_{29}F_3N_7O_2$, 468.2329; found: 468.2311. **HPLC**: t_R = 9.72 min (97.2% purity).

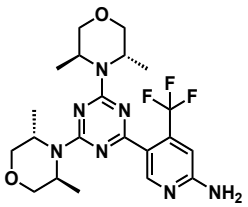

5-{4,6-Bis[(3*S*,5*S*)-3,5-dimethylmorpholin-4-yl]-1,3,5-triazin-2-yl}-4-(trifluoromethyl)pyridin-2-amine (21). Compound **21** was prepared according to general procedure 1 from intermediate **14** (185 mg, 541 µmol, 1.0 equiv) and boronic acid pinacol ester **48** (205 mg, 597 µmol, 1.1 equiv). Purification by column chromatography on silica gel (cyclohexane / ethyl acetate 1:0 → 7:3) gave compound **21** as a colorless solid (143 mg, 306 µmol, 57%). **^{1}H NMR** (400 MHz, $CDCl_3$): δ 8.77 (s, 1 H), 6.79 (s, 1 H), 4.82 (br s, 2 H), 4.45-4.34 (m, 4 H), 4.23 (dd, $^2J_{H,H}$ = 11 Hz, $^3J_{H,H}$ = 3.3 Hz, 4 H), 3.74 (dd, $^2J_{H,H}$ = 11 Hz, $^3J_{H,H}$ = 2.3 Hz, 4 H), 1.46 (d, $^3J_{H,H}$ = 6.6 Hz, 12 H). **^{19}F{^{1}H} NMR** (376 MHz, $CDCl_3$): δ − 60.4 (s, 3 F). **^{13}C{^{1}H} NMR** (101 MHz, $CDCl_3$): δ 169.4 (s, 1 C), 164.1 (s, 2 C), 159.4 (s, 1 C), 153.1 (s, 1 C), 138.3 (q, $^2J_{C,F}$ = 33 Hz, 1 C), 123.0 (q, $^1J_{C,F}$ = 274 Hz, 1 C), 122.8 (s, 1 C), 105.5-105.1 (m, 1 C), 68.0 (s, 4 C), 48.0 (s, 4 C), 19.8 (s, 4 C). **NSI-HRMS** (*m/z*): $[M + H]^+$ calc. for $C_{21}H_{29}F_3N_7O_2$, 468.2329; found: 468.2321. **HPLC**: t_R = 9.30 min (98.6% purity).

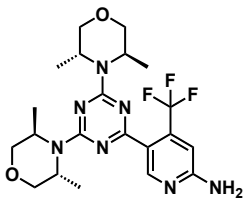

5-{4,6-Bis[(3*R*,5*R*)-3,5-dimethylmorpholin-4-yl]-1,3,5-triazin-2-yl}-4-(trifluoromethyl)pyridin-2-amine (22). Compound **22** was prepared according to general procedure 1 from intermediate **15** (229 mg, 670 µmol, 1.0 equiv) and boronic acid pinacol ester **48** (250 mg, 729 µmol, 1.1 equiv). Purification by column chromatography on silica gel (cyclohexane / ethyl acetate 1:0 → 6:4) gave compound **22** as a yellowish solid (110 mg, 235 µmol, 35%). **^{1}H NMR** (400 MHz, $CDCl_3$): δ 8.77 (s, 1 H), 6.79 (s, 1 H), 4.83 (br s, 2 H), 4.46-4.34 (m, 4 H), 4.23 (dd, $^2J_{H,H}$ = 11 Hz, $^3J_{H,H}$ = 3.3 Hz, 4 H), 3.74 (dd, $^2J_{H,H}$ = 11 Hz, $^3J_{H,H}$ = 2.2 Hz, 4 H), 1.45 (d, $^3J_{H,H}$ = 6.6 Hz, 12 H). **^{19}F{^{1}H} NMR** (376 MHz, $CDCl_3$): δ − 60.4 (s, 3 F). **^{13}C{^{1}H} NMR** (101 MHz, $CDCl_3$): δ 169.4 (s, 1 C), 164.1 (s, 2 C), 159.4 (s, 1 C), 153.1 (s, 1 C), 138.3 (q, $^2J_{C,F}$ = 33 Hz, 1 C), 123.0 (q, $^1J_{C,F}$ =274 Hz, 1 C), 122.8 (s, 1 C), 105.5-105.0 (m, 1 C), 68.0 (s, 4 C), 48.0 (s, 4 C), 19.8 (s, 4 C). **NSI-HRMS** (*m/z*): $[M + H]^+$ calc. for $C_{21}H_{29}F_3N_7O_2$, 468.2329; found: 468.2313. **HPLC**: t_R = 9.31 min (96.2% purity).

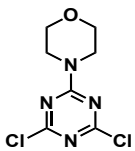

2,4-Dichloro-6-(morpholin-4-yl)-1,3,5-triazine (23). Compound **23** was prepared according to the literature.[9]

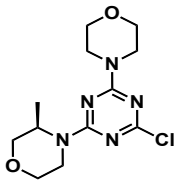

2-Chloro-4-[(3*R*)-3-methylmorpholin-4-yl]-6-(morpholin-4-yl)-1,3,5-triazine (24). Compound **24** was prepared according to the literature.[17]

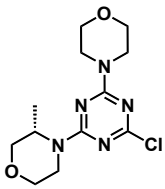

2-Chloro-4-[(3*S*)-3-methylmorpholin-4-yl]-6-(morpholin-4-yl)-1,3,5-triazine (25). To a solution of (*S*)-3-methylmorpholine (560 mg, 5.54 mmol, 1.2 equiv) and *N*,*N*-diisopropylethylamine (1.70 mL, 9.76 mmol, 2.1 equiv) in ethanol (10 mL) at 0 °C, 4-(4,6-dichloro-1,3,5-triazin-2-yl)morpholine (**23**, 1.11 g, 4.72 mmol, 1.0 equiv) was added portionwise. The resulting mixture was stirred at room temperature overnight. The solvent was removed under reduced pressure and the residue was purified by column chromatography on silica gel (cyclohexane / ethyl acetate 1:0 → 4:1) to afford compound **25** as a colorless solid (1.46 g, 4.87 mmol, 74%). **^{1}H NMR** (400 MHz, $CDCl_3$): δ 4.75-4.57 (m, 1 H), 4.40-4.23 (m, 1 H), 3.93 (dd, $J_{H,H}$ = 11, 3.8 Hz, 1 H), 3.85-3.67 (m, 9 H), 3.63 (dd, $J_{H,H}$ = 11, 3.2 Hz, 1 H), 3.48 (td, $J_{H,H}$ = 12, 2.9 Hz, 1 H), 3.29-3.20 (m, 1 H), 1.30 (d, $^3J_{H,H}$ = 6.9 Hz, 3 H). **^{13}C{^{1}H} NMR** (101 MHz, $CDCl_3$): δ 169.8 (s, 1 C), 164.6 (s, 1 C), 164.3 (s, 1 C), 71.0 (s, 1 C), 66.9 (s, 1 C), 66.7 (br s, 2 C), 46.8 (s, 1 C), 43.9 (s, 2 C), 38.9 (s, 1 C), 14.5 (br s, 1 C). **MALDI-MS**: *m/z* = 300.3 ([M + H]$^+$).

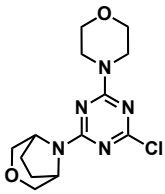

8-[4-Chloro-6-(morpholin-4-yl)-1,3,5-triazin-2-yl]-3-oxa-8-azabicyclo[3.2.1]octane (26). Compound **26** was prepared according to the literature.[17]

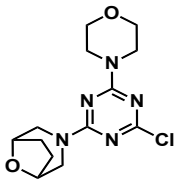

3-[4-Chloro-6-(morpholin-4-yl)-1,3,5-triazin-2-yl]-8-oxa-3-azabicyclo[3.2.1]octane (27). Compound **27** was prepared according to the literature.[17]

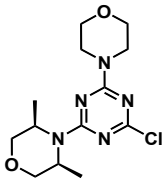

2-Chloro-4-[(3*R*,5*S*)-3,5-dimethylmorpholin-4-yl]-6-(morpholin-4-yl)-1,3,5-triazine (28). Compound **28** was prepared according to general procedure 2 from (3*R*,5*S*)-3,5-dimethylmorpholine (160 mg, 1.39 mmol, 1.1 equiv) and 4-(4,6-dichloro-1,3,5-triazin-2-yl)morpholine (**23**, 304 mg, 1.29 mmol, 1.0 equiv) in presence of *N*,*N*-diisopropylethylamine (1.05 mL, 6.03 mmol, 4.7 equiv). Purification by column chromatography on silica gel (cyclohexane / ethyl acetate 1:0 → 4:1) gave compound **28** as a colorless solid (297 mg, 1.39 mmol, 73%). **^{1}H NMR** (400 MHz, $CDCl_3$): δ 4.55-4.43 (m, 2 H), 3.81-3.73 (m, 6 H), 3.71-3.67 (m, 4 H), 3.59 (dd, $^2J_{H,H}$ = 12 Hz, $^3J_{H,H}$ = 3.9 Hz, 2 H), 1.34 (d, $^3J_{H,H}$ = 7.0 Hz, 6 H). **^{13}C{^{1}H} NMR** (101 MHz, $CDCl_3$): δ 169.7 (s, 1 C), 164.6 (s, 1 C), 164.1 (s, 1 C), 71.3 (s, 2 C), 66.7 (br s, 2 C), 46.2 (s, 2 C), 43.9 (s, 2 C), 19.1 (br s, 2 C). **MALDI-MS**: *m/z* = 314.2 ($[M + H]^+$).

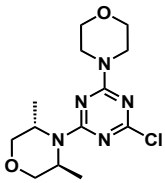

2-Chloro-4-[(3S,5S)-3,5-dimethylmorpholin-4-yl]-6-(morpholin-4-yl)-1,3,5-triazine (29). Compound **29** was prepared according to general procedure 2 from (3*S*,5*S*)-3,5-dimethylmorpholine (182 mg, 1.58 mmol, 1.2 equiv) and 4-(4,6-dichloro-1,3,5-triazin-2-yl)morpholine (**23**, 304 mg, 1.29 mmol, 1.0 equiv) in presence of *N*,*N*-diisopropylethylamine (1.00 mL, 5.74 mmol, 4.5 equiv). Purification by column chromatography on silica gel (cyclohexane / ethyl acetate 1:0 → 4:1) gave compound **29** as a colorless solid (351 mg, 1.12 mmol, 87%). **^{1}H NMR** (400 MHz, $CDCl_3$): δ 4.35-4.26 (m, 2 H), 4.19 (dd, $^2J_{H,H}$ = 11 Hz, $^3J_{H,H}$ = 3.3 Hz, 2 H), 3.85-3.68 (m, 8 H), 1.41 (d, $^3J_{H,H}$ = 6.7 Hz, 6 H). **^{13}C{^{1}H} NMR** (101 MHz, $CDCl_3$): δ 169.4 (s, 1 C), 164.5 (s, 1 C), 164.2 (s, 1 C), 67.6 (s, 2 C), 66.8 (br s, 2 C), 48.4 (s, 2 C), 44.0 (s, 2 C), 19.6 (s, 2 C). **MALDI-MS**: *m/z* = 314.2 ($[M + H]^+$).

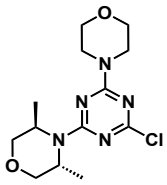

2-Chloro-4-[(3*R*,5*R*)-3,5-dimethylmorpholin-4-yl]-6-(morpholin-4-yl)-1,3,5-triazine (30). Compound **30** was prepared according to general procedure 2 from (3*R*,5*R*)-3,5-dimethylmorpholine (250 mg, 2.17 mmol, 1.2 equiv) and 4-(4,6-dichloro-1,3,5-triazin-2-yl)morpholine (**23**, 434 mg, 1.85 mmol, 1.0 equiv) in presence of *N*,*N*-diisopropylethylamine (1.50 mL, 8.61 mmol, 4.7 equiv). Purification by column chromatography on silica gel (cyclohexane / ethyl acetate 1:0 → 4:1) gave compound **30** as a colorless solid (504 mg, 1.61 mmol, 87%). **^{1}H NMR** (400 MHz, $CDCl_3$): δ 4.35-4.25 (m, 2 H), 4.17 (dd, $^2J_{H,H}$ = 11 Hz, $^3J_{H,H}$ = 3.3 Hz, 2 H), 3.84-3.64 (m, 10 H), 1.40 (d, $^3J_{H,H}$ = 6.7 Hz, 6 H). **^{13}C{^{1}H} NMR** (101 MHz, $CDCl_3$): δ 169.4 (s, 1 C), 164.4 (s, 1 C), 164.1 (s, 1 C), 67.5 (s, 2 C), 66.7 (br s, 2 C), 48.4 (s, 2 C), 43.9 (br s, 2 C), 19.5 (br s, 2 C). **MALDI-MS**: *m/z* = 314.3 ([M + H]$^+$).

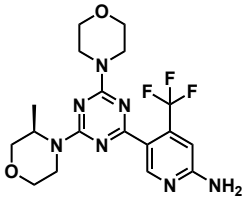

5-{4-[(3*R*)-3-Methylmorpholin-4-yl]-6-(morpholin-4-yl)-1,3,5-triazin-2-yl}-4-(trifluoromethyl)pyridin-2-amine (**31**). Compound **31** was prepared according to general procedure 1 from intermediate **24** (100 mg, 334 µmol, 1.0 equiv) and boronic acid pinacol ester **48** (130 mg, 379 µmol, 1.1 equiv). Purification by column chromatography on silica gel (cyclohexane / ethyl acetate 1:0 → 3:7) gave compound **31** as a colorless solid (45.5 mg, 107 µmol, 32%). **^{1}H NMR** (400 MHz, $CDCl_3$): δ 8.72 (s, 1 H), 6.79 (s, 1 H), 4.92-4.71 (m, 3 H), 4.52-4.32 (m, 1 H), 4.04-3.91 (m, 1 H), 3.91-3.79 (m, 4 H), 3.77-3.63 (m, 6 H), 3.57-3.46 (m, 1 H), 3.32-3.20 (m, 1 H), 1.32 (d, $^3J_{H,H}$ = 6.8 Hz, 3 H). **^{19}F{^{1}H} NMR** (376 MHz, $CDCl_3$): δ − 60.2 (s, 3 F). **^{13}C{^{1}H} NMR** (101 MHz, $CDCl_3$): δ 170.0 (s, 1 C), 164.9 (s, 1 C), 164.5 (s, 1 C), 159.6 (s, 1 C), 152.8 (s, 1 C), 138.5 (q, $^2J_{C,F}$ = 33 Hz, 1 C), 123.0 (q, $^1J_{C,F}$ = 274 Hz, 1 C), 122.5 (br s, 1 C), 105.5 (q, $^3J_{C,F}$ = 6.1 Hz, 1 C), 71.2 (s, 1 C), 67.2 (s, 1 C), 66.9 (br s, 2 C),

46.4 (s, 1 C), 43.7 (br s, 2 C), 38.6 (s, 1 C), 14.4 (s, 1 C). **NSI-HRMS** (*m/z*): $[M + H]^+$ calc. for $C_{18}H_{23}F_3N_7O_2$, 426.1860; found: 426.1856. **HPLC**: t_R = 7.96 min (96.4% purity).

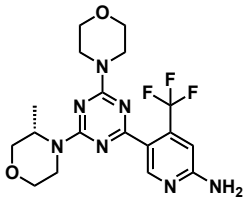

5-{4-[(3*S*)-3-Methylmorpholin-4-yl]-6-(morpholin-4-yl)-1,3,5-triazin-2-yl}-4-(trifluoromethyl)pyridin-2-amine (32). Compound **32** was prepared according to general procedure 1 from intermediate **25** (80.0 mg, 268 µmol, 1.0 equiv) and boronic acid pinacol ester **48** (94.0 mg, 273 µmol, 1.0 equiv). Purification by column chromatography on silica gel (cyclohexane / ethyl acetate 1:0 → 3:7) gave compound **32** as a colorless solid (84.1 mg, 198 µmol, 74%). **^{1}H NMR** (400 MHz, $CDCl_3$): δ 8.72 (s, 1 H), 6.79 (s, 1 H), 4.90-4.71 (m, 3 H), 4.50-4.33 (m, 1 H), 3.95 (dd, $J_{H,H}$ = 11, 3.7 Hz, 1 H), 3.90-3.70 (m, 9 H), 3.67 (dd, $J_{H,H}$ = 12, 3.2 Hz, 1 H), 3.51 (td, $J_{H,H}$ = 12, 3.0 Hz, 1 H), 3.26 (td, $J_{H,H}$ = 13, 3.8 Hz, 1 H), 1.31 (d, $^3J_{H,H}$ = 6.8 Hz, 3 H). **^{19}F{^{1}H} NMR** (376 MHz, $CDCl_3$): δ − 59.9 (s, 3 F). **^{13}C{^{1}H} NMR** (101 MHz, $CDCl_3$): δ 170.0 (s, 1 C), 164.9 (s, 1 C), 164.5 (s, 1 C), 159.6 (s, 1 C), 152.9 (s, 1 C), 138.5 (q, $^2J_{C,F}$ = 33 Hz, 1 C), 123.0 (q, $^1J_{C,F}$ = 274 Hz, 1 C), 122.6 (s, 1 C), 105.4 (q, $^3J_{C,F}$ = 4.9 Hz, 1 C), 71.2 (s, 1 C), 67.2 (s, 1 C), 66.9 (br s, 2 C), 46.4 (s, 1 C), 43.7 (br s, 2 C), 38.6 (s, 1 C), 14.4 (s, 1 C). **NSI-HRMS** (*m/z*): $[M + H]^+$ calc. for $C_{18}H_{23}F_3N_7O_2$, 426.1860; found: 426.1850. **HPLC**: t_R = 7.96 min (96.9% purity).

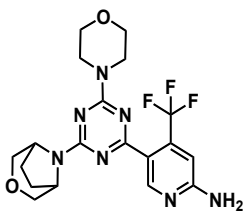

5-[4-(Morpholin-4-yl)-6-{3-oxa-8-azabicyclo[3.2.1]octan-8-yl}-1,3,5-triazin-2-yl]-4-(trifluoromethyl)pyridin-2-amine (**33**). Compound **33** was prepared according to general procedure

1 from intermediate **26** (80.0 mg, 257 µmol, 1.0 equiv) and boronic acid pinacol ester **48** (90.0 mg, 262 µmol, 1.0 equiv). Purification by column chromatography on silica gel (cyclohexane / ethyl acetate 1:0 → 3:7) gave compound **33** as a colorless solid (52.1 mg, 119 µmol, 46%). **^{1}H NMR** (400 MHz, $CDCl_3$): δ 8.72 (s, 1 H), 6.78 (s, 1 H), 4.85 (br s, 2 H), 4.77-4.71 (m, 1 H), 4.68-4.63 (m, 1 H), 3.93-3.69 (m, 10 H), 3.63 (dd, $^2J_{H,H}$ = 11 Hz, $J_{H,H}$ = 1.2 Hz, 2 H), 2.13-1.92 (m, 4 H). **^{19}F{^{1}H} NMR** (376 MHz, $CDCl_3$): δ − 59.8 (s, 3 F). **^{13}C{^{1}H} NMR** (101 MHz, $CDCl_3$): δ 170.2 (s, 1 C), 165.0 (s, 1 C), 163.1 (s, 1 C), 159.7 (s, 1 C), 152.7 (s, 1 C), 138.5 (q, $^2J_{C,F}$ = 33 Hz, 1 C), 123.0 (q, $^1J_{C,F}$ = 274 Hz, 1 C), 122.3 (br s, 1 C), 105.5 (q, $^3J_{C,F}$ = 5.7 Hz, 1 C), 72.1 (s, 1 C), 71.7 (s, 1 C), 66.9 (s, 2 C), 54.9 (s, 1 C), 54.5 (s, 1 C), 43.7 (s, 2 C), 27.0 (s, 2 C). **NSI-HRMS** (*m/z*): [M + H]$^+$ calc. for $C_{19}H_{23}F_3N_7O_2$, 438.1860; found: 438.1840. **HPLC**: t_R = 7.59 min (96.6% purity).

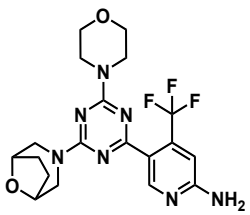

5-[4-(Morpholin-4-yl)-6-{8-oxa-3-azabicyclo[3.2.1]octan-3-yl}-1,3,5-triazin-2-yl]-4-(trifluoromethyl)pyridin-2-amine (34). Compound **34** was prepared according to general procedure 1 from intermediate **27** (80.0 mg, 257 µmol, 1.0 equiv) and boronic acid pinacol ester **48** (90.0 mg, 262 µmol, 1.0 equiv). Purification by column chromatography on silica gel (cyclohexane / ethyl acetate 1:0 → 3:7) gave compound **34** as a colorless solid (64.3 mg, 147 µmol, 57%). **^{1}H NMR** (400 MHz, $CDCl_3$): δ 8.70 (s, 1 H), 6.77 (s, 1 H), 4.91 (br s, 1 H), 4.91 (br s, 2 H), 4.48-4.38 (m, 3 H), 4.31 (d, $^2J_{H,H}$ = 13 Hz, 1 H), 3.89-3.77 (m, 4 H), 3.76-3.69 (m, 4 H), 3.18 (d, $^2J_{H,H}$ = 13 Hz, 1 H), 1.98-1.87 (m, 2 H), 1.82-1.72 (m, 2 H). **^{19}F{^{1}H} NMR** (376 MHz, $CDCl_3$): δ − 59.8 (s, 3 F). **^{13}C{^{1}H} NMR** (101 MHz, $CDCl_3$): δ 169.8 (s, 1 C), 165.9 (s, 1 C), 164.7 (s, 1 C), 159.6 (s, 1 C), 152.8 (s, 1 C), 138.5 (q, $^2J_{C,F}$ = 33 Hz, 1 C), 123.0 (q, $^1J_{C,F}$ = 274 Hz, 1 C), 122.6-122.5 (m, 1 C), 105.4 (q, $^3J_{C,F}$ = 5.9 Hz, 1 C), 74.1 (s, 1 C), 74.0 (s, 1 C), 66.9 (s, 2 C), 49.4 (s, 1 C), 49.1 (s, 1 C), 43.7 (br s, 2 C), 27.7 (s, 1 C), 27.6 (s, 1 C). **NSI-HRMS** (*m/z*): [M + H]$^+$ calc. for $C_{19}H_{23}F_3N_7O_2$, 438.1860; found: 438.1851. **HPLC**: t_R = 7.46 min (99.0% purity).

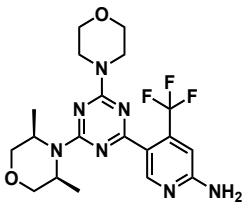

5-{4-[(3*R*,5*S*)-3,5-Dimethylmorpholin-4-yl]-6-(morpholin-4-yl)-1,3,5-triazin-2-yl}-4-(trifluoromethyl)pyridin-2-amine (35). Compound **35** was prepared according to general procedure 1 from intermediate **28** (200 mg, 637 µmol, 1.0 equiv) and boronic acid pinacol ester **48** (222 mg, 647 µmol, 1.0 equiv). Purification by column chromatography on silica gel (cyclohexane / ethyl acetate 1:0 → 1:4) gave compound **35** as a colorless solid (60.1 mg, 137 µmol, 21%). **^{1}H NMR** (400 MHz, $CDCl_3$): δ 8.74 (s, 1 H), 6.79 (s, 1 H), 4.84 (br s, 2 H), 4.71-4.53 (m, 2 H), 3.94-3.70 (m, 10 H), 3.67-3.59 (m, 2 H), 1.37 (d, $^3J_{H,H}$ = 6.9 Hz, 6 H). **^{19}F{^{1}H} NMR** (376 MHz, $CDCl_3$): δ − 60.2 (s, 3 F); **^{13}C{^{1}H} NMR** (101 MHz, $CDCl_3$): δ 169.8 (s, 1 C), 164.9 (s, 1 C), 164.1 (s, 1 C), 159.6 (s, 1 C), 152.9 (s, 1 C), 138.4 (q, $^2J_{C,F}$ = 33 Hz, 1 C), 123.0 (q, $^1J_{C,F}$ = 274 Hz, 1 C), 122.5 (s, 1 C), 105.8-105.0 (m, 1 C), 71.5 (s, 2 C), 66.9 (br s, 2 C), 45.7 (s, 2 C), 43.7 (br s, 2 C), 19.2 (s, 2 C). **NSI-HRMS** (*m/z*): $[M + H]^+$ calc. for $C_{19}H_{25}F_3N_7O_2$, 440.2016; found: 440.1998. **HPLC**: t_R = 8.62 min (98.8% purity).

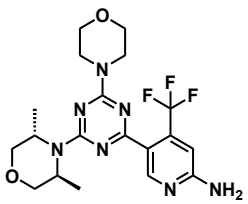

5-{4-[(3*S*,5*S*)-3,5-Dimethylmorpholin-4-yl]-6-(morpholin-4-yl)-1,3,5-triazin-2-yl}-4-(trifluoromethyl)pyridin-2-amine (36). Compound **36** was prepared according to general procedure 1 from intermediate **29** (200 mg, 637 µmol, 1.0 equiv) and boronic acid pinacol ester **48** (222 mg, 647 µmol, 1.0 equiv). Purification by column chromatography on silica gel (cyclohexane / ethyl acetate 1:0 → 1:4) gave compound **36** as a yellowish solid (160 mg, 364 µmol, 57%). **^{1}H NMR** (400 MHz, $CDCl_3$): δ 8.75 (s, 1 H), 6.79 (s, 1 H), 4.84 (br s, 2 H), 4.46-4.35 (m 2 H), 4.22 (dd, $^2J_{H,H}$ = 11 Hz, $^3J_{H,H}$ = 3.2 Hz, 2 H), 3.91-3.79 (m, 4 H), 3.78-3.69 (m, 6 H), 1.43 (d, $^3J_{H,H}$ = 6.6 Hz, 6 H). **^{19}F{^{1}H} NMR** (376 MHz, $CDCl_3$): δ − 60.2(s, 3 F). **^{13}C{^{1}H} NMR** (101 MHz, $CDCl_3$): δ 169.6 (s, 1 C), 164.6 (s, 1 C),

164.2 (s, 1 C), 159.4 (s, 1 C), 152.8 (s, 1 C), 138.3 (q, $^{2}J_{C,F}$ = 33 Hz, 1 C), 122.7 (q, $^{1}J_{C,F}$ = 274 Hz, 1 C), 122.5 (s, 1 C), 105.3 (q, $^{3}J_{C,F}$ = 6.0 Hz, 1 C), 67.9 (s, 2 C), 66.8 (br s, 2 C), 47.9 (s, 2 C), 43.6 (br s, 2 C), 19.5 (s, 2 C). **NSI-HRMS** (*m/z*): $[M + H]^+$ calc. for $C_{19}H_{25}F_3N_7O_2$, 440.2016; found: 440.2002. **HPLC**: t_R = 8.48 min (97.5% purity).

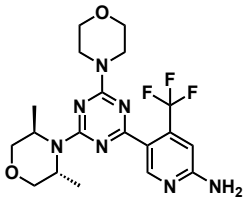

5-{4-[(3*R*,5*R*)-3,5-Dimethylmorpholin-4-yl]-6-(morpholin-4-yl)-1,3,5-triazin-2-yl}-4-(trifluoromethyl)pyridin-2-amine (37). Compound **37** was prepared according to general procedure 1 from intermediate **30** (175 mg, 558 µmol, 1.0 equiv) and boronic acid pinacol ester **48** (210 mg, 612 µmol, 1.1 equiv). Purification by column chromatography on silica gel (cyclohexane / ethyl acetate 1:0 → 2:3) gave compound **37** as a colorless solid (111 mg, 253 µmol, 45%). **^{1}H NMR** (400 MHz, $CDCl_3$): δ 8.75 (s, 1 H), 6.79 (s, 1 H), 4.83 (br s, 2 H), 4.47-4.34 (m 2 H), 4.22 (dd, $^{2}J_{H,H}$ = 11 Hz, $^{3}J_{H,H}$ = 3.4 Hz, 2 H), 3.94-3.79 (m, 4 H), 3.79-3.69 (m, 6 H), 1.43 (d, $^{3}J_{H,H}$ = 6.6 Hz, 6 H). **^{19}F{^{1}H} NMR** (376 MHz, $CDCl_3$): δ − 60.2(s, 3 F). **^{13}C{^{1}H} NMR** (101 MHz, $CDCl_3$): δ 169.7 (s, 1 C), 164.7 (s, 1 C), 164.4 (s, 1 C), 159.6 (s, 1 C), 152.9 (s, 1 C), 138.4 (q, $^{2}J_{C,F}$ = 33 Hz, 1 C), 122.9 (q, $^{1}J_{C,F}$ = 274 Hz, 1 C), 122.5 (br s, 1 C), 105.4 (q, $^{3}J_{C,F}$ = 5.7 Hz, 1 C), 68.0 (s, 2 C), 66.9 (br s, 2 C), 48.0 (s, 2 C), 43.7 (br s, 2 C), 19.7 (s, 2 C). **NSI-HRMS** (*m/z*): $[M + H]^+$ calc. for $C_{19}H_{25}F_3N_7O_2$, 440.2016; found: 440.2004. **HPLC:** t_R = 8.48 min (99.2% purity).

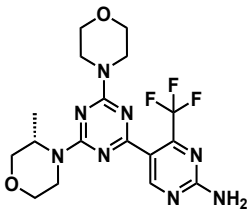

5-{4-[(3*S*)-3-Methylmorpholin-4-yl]-6-(morpholin-4-yl)-1,3,5-triazin-2-yl}-4-(trifluoromethyl)pyrimidin-2-amine (38). Intermediate **25** (100 mg, 334 µmol, 1.0 equiv), 2-amino-

4-trifluoromethylpyrimidine-5-boronic acid pinacol ester (106 mg, 367 µmol, 1.1 equiv), phosphate tribasic (142 mg, 669 µmol, 2.0 equiv) and chloro(2-dicyclohexylphosphino-2′,4′,6′-triisopropyl-1,1′-biphenyl)[2-(2′-amino-1,1′-biphenyl)]palladium(II) (XPhos Pd G2, 13.0 mg, 16.5 µmol, 0.05 equiv) were charged in a flask. Under nitrogen atmosphere, absolute 1,4-dioxane (2.5 mL) and deionized H_2O (0.8 mL) were added and the resulting mixture was directly placed into an oil bath pre-heated at 95 °C and allowed to stir at this temperature for 2 hours. Then, the reaction mixture was allowed to cool down to room temperature. Brine was added and the aqueous layer was extracted with ethyl acetate (3 x). The combined organic layer was washed with a 2 M aqueous NaOH-solution, dried over anhydrous Na_2SO_4, filtered and the solvent was rotatory evaporated under reduced pressure. The crude product was purified by column chromatography on silica gel (cyclohexane / ethyl acetate 4:1 → 3:2) to obtain compound **38** as a colorless solid (88.2 mg, 207 µmol, 62%). **^{1}H NMR** (400 MHz, $CDCl_3$): δ 8.95 (s, 1 H), 5.49 (br s, 2 H), 4.84-4.67 (m, 1 H), 4.50-4.32 (m, 1 H), 3.95 (dd, $^2J_{H,H}$ = 11 Hz, $^3J_{H,H}$ = 3.4 Hz, 1 H), 3.92-3.79 (m, 4 H), 3.79-3.62 (m, 6 H), 3.51 (td, $J_{H,H}$ = 12, 2.8 Hz, 1 H), 3.26 (td, $J_{H,H}$ = 13, 3.8 Hz, 1 H), 1.32 (d, $^3J_{H,H}$ = 6.8 Hz, 3 H). **^{19}F{^{1}H} NMR** (376 MHz, $CDCl_3$): δ − 65.0 (s, 3 F). **^{13}C{^{1}H} NMR** (101 MHz, $CDCl_3$): δ 168.5 (s, 1 C), 164.8 (s, 1 C), 164.4 (s, 1 C), 163.1 (s, 1 C), 162.7 (s, 1 C), 154.5 (q, $^2J_{C,F}$ = 35 Hz, 1 C), 121.0 (s, 1 C), 120.8 (q, $^1J_{C,F}$ = 276 Hz, 1 C), 71.1 (s, 1 C), 67.1 (s, 1 C), 66.9 (br s, 2 C), 46.5 (s, 1 C), 43.7 (br s, 2 C), 38.6 (s, 1 C), 14.3 (br s, 1 C). **NSI-HRMS** (*m/z*): $[M + H]^+$ calc. for $C_{17}H_{22}F_3N_8O_2$, 427.1812; found: 427.1797. **HPLC**: t_R = 8.04 min (98.5% purity).

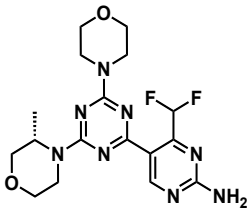

4-(Difluoromethyl)-5-{4-[(3*S*)-3-methylmorpholin-4-yl]-6-(morpholin-4-yl)-1,3,5-triazin-2-yl}pyrimidin-2-amine (39). Compound **39** was prepared according to general procedure 3 from intermediate **25** (100 mg, 334 µmol, 1.1 equiv) and compound **52** (129 mg, 304 µmol, 1.0 equiv). Purification by column chromatography on silica gel (cyclohexane / ethyl acetate 1:0 → 3:2) gave compound **39** as a colorless solid (74.0 mg, 181 µmol, 60%). **^{1}H NMR** (400 MHz, $CDCl_3$): δ 9.23 (s, 1

H), 7.64 (t, $^{2}J_{H,F}$ = 54 Hz, 1 H), 5.65 (br s, 2 H), 4.78-4.68 (m, 1 H), 4.44-4.33 (m, 1 H), 4.02-3.94 (m, 1 H), 3.90-3.72 (m, 9 H), 3.67 (dd, $^{2}J_{H,H}$ = 12 Hz, $^{3}J_{H,H}$ = 3.3 Hz, 1 H), 3.52 (td, $J_{H,H}$ = 12, 3.0 Hz, 1 H), 3.34-3.21 (m, 1 H), 1.33 (d, $^{3}J_{H,H}$ = 6.9 Hz, 3 H). **^{19}F{^{1}H} NMR** (376 MHz, $CDCl_3$): δ − 121.5 (s, 2 F). **^{13}C{^{1}H} NMR** (101 MHz, $CDCl_3$): δ 167.8 (s, 1 C), 164.7 (s, 1 C), 164.3 (s, 1 C), 163.7 (s, 1 C), 162.6 (s, 1 C), 159.6 (t, $^{2}J_{C,F}$ = 21 Hz, 1 C), 119.8 (s, 1 C), 109.6 (t, $^{1}J_{C,F}$ = 240 Hz, 1 C), 71.1 (s, 1 C), 67.1 (s, 1 C), 66.9 (s, 2 C), 46.6 (s, 1 C), 43.8 (br s, 2 C), 38.7 (s, 1 C), 14.4 (s, 1 C). **NSI-HRMS** (*m/z*): [M + H]$^{+}$ calc. for $C_{17}H_{23}F_2N_8O_2$, 409.1907; found: 409.1891. **HPLC**: t_R = 7.53 min (> 99.9% purity).

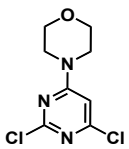

4-(2,6-Dichloropyrimidin-4-yl)morpholine (40). Compound **40** was prepared according to the literature.[9]

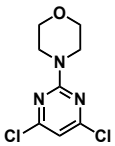

4-(4,6-Dichloropyrimidin-2-yl)morpholine (41). Compound **41** was prepared according to the literature.[9]

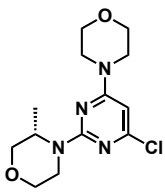

(3*S*)-4-[4-Chloro-6-(morpholin-4-yl)pyrimidin-2-yl]-3-methylmorpholine (42). Compound **42** was prepared according to general procedure 4 from (*S*)-3-methylmorpholine (450 mg, 4.45 mmol, 1.5 equiv) and 4-(2,6-dichloropyrimidin-4-yl)morpholine (**40**, 694 mg, 2.96 mmol, 1.0 equiv) in presence of *N*,*N*-diisopropylethylamine (1.54 mL, 8.84 mmol, 3.0 equiv). Purification by column chromatography on silica gel (cyclohexane / ethyl acetate 3:1 → 1:1) gave compound **42** as a colorless

solid (475 mg, 1.59 mmol, 54%). **^{1}H NMR** (400 MHz, $CDCl_3$): δ 5.85 (s, 1 H), 4.66-4.57 (m, 1 H), 4.25 (dd, $J_{H,H}$ = 13, 2.8 Hz 1 H), 3.93 (dd, $J_{H,H}$ = 11, 3.7 Hz 1 H), 3.78-3.70 (m, 5 H), 3.65 (dd, $J_{H,H}$ = 11, 3.1 Hz, 1 H), 3.57-3.51 (m, 4 H), 3.48 (dd, $J_{H,H}$ = 11, 3.0 Hz, 1 H), 3.27-3.17 (m, 1 H), 1.26 (d, $^3J_{H,H}$ = 6.8 Hz, 3 H). **^{13}C{^{1}H} NMR** (101 MHz, $CDCl_3$): δ 163.7 (s, 1 C), 160.7 (s, 1 C), 160.5 (s, 1 C), 91.1 (s, 1 C), 71.3 (s, 1 C), 67.2 (s, 1 C), 66.6 (s, 2 C), 46.9 (s, 1 C), 44.5 (s, 2 C), 39.2 (s, 1 C), 13.9 (s, 1 C). **MALDI-MS**: *m/z* = 299.2 ([M + H]$^+$).

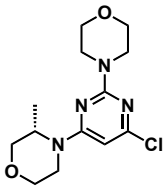

(3*S*)-4-[6-Chloro-2-(morpholin-4-yl)pyrimidin-4-yl]-3-methylmorpholine (43). Compound **43** was prepared according to general procedure 4 from (*S*)-3-methylmorpholine (194 mg, 1.92 mmol, 1.5 equiv) and 4-(4,6-dichloropyrimidin-2-yl)morpholine (**41**, 300 mg, 1.28 mmol, 1.0 equiv) in the presence of *N*,*N*-diisopropylethylamine (670 µl, 3.84 mmol, 3.0 equiv). Purification by column chromatography on silica gel (cyclohexane / ethyl acetate 1:0 → 4:1) gave compound **43** as a colorless solid (267 mg, 894 µmol, 70%). **^{1}H NMR** (400 MHz, $CDCl_3$): δ 5.84 (s, 1 H), 4.24-4.14 (m, 1 H), 4.00-3.86 (m, 2 H), 3.79-3.64 (m, 10 H), 3.53 (td, $J_{H,H}$ = 12, 3.1 Hz, 1 H), 3.21 (td, $J_{H,H}$ = 13, 3.9 Hz, 1 H), 1.27 (d, $^3J_{H,H}$ = 6.8 Hz, 3 H). **^{13}C{^{1}H} NMR** (101 MHz, $CDCl_3$): δ 163.0 (s, 1 C), 161.0 (s, 1 C), 160.6 (s, 1 C), 91.2 (s, 1 C), 71.0 (s, 1 C), 66.9 (s, 2 C), 66.8 (s, 1 C), 47.4 (s, 1 C), 44.4 (s, 2 C), 39.3 (s, 1 C), 13.7 (s, 1 C). **MALDI-MS**: *m/z* = 299.2 ([M + H]$^+$).

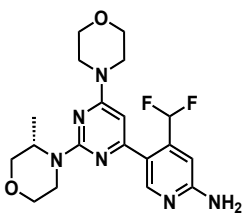

4-(Difluoromethyl)-5-{2-[(3S)-3-methylmorpholin-4-yl]-6-(morpholin-4-yl)pyrimidin-4-yl}pyridin-2-amine (44). Compound **44** was prepared according to general procedure 1 from intermediate **42**

(73.5 mg, 246 µmol, 1.0 equiv) and boronic acid pinacol ester **49** (80.0 mg, 246 µmol, 1.0 equiv). Purification by column chromatography on silica gel (ethyl acetate / MeOH 1:0 → 100:2) gave compound **44** as a colorless solid (57.3 mg, 141 µmol, 57%). **^{1}H NMR** (400 MHz, $CDCl_3$): δ 8.31 (s, 1 H), 7.32 (t, $^2J_{H,F}$ = 55 Hz, 1 H), 6.85 (s, 1 H), 6.04 (s, 1 H), 4.75-4.63 (m, 3 H), 4.29 (dd, $^2J_{H,H}$ = 13 Hz, $^3J_{H,H}$ = 2.1 Hz, 1 H), 3.96 (dd, $J_{H,H}$ = 11, 3.4 Hz, 1 H), 3.82-3.66 (m, 6 H), 3.66-3.49 (m, 5 H), 3.25 (td, $J_{H,H}$ = 13, 3.7 Hz, 1 H), 1.29 (d, $^3J_{H,H}$ = 6.9 Hz, 3 H). **^{19}F{^{1}H} NMR** (376 MHz, $CDCl_3$): δ − 113.7-(− 117.9) (m, 2 F). **^{13}C{^{1}H} NMR** (101 MHz, $CDCl_3$): δ 163.8 (s, 1 C), 162.7 (s, 1 C), 161.0 (s, 1 C), 159.2 (s, 1 C), 149.2 (s, 1 C),142.6 (t, $^2J_{C,F}$ = 22 Hz, 1 C), 124.7 (t, $^3J_{C,F}$ = 5.2 Hz, 1 C), 111.6 (t, $^1J_{C,F}$ = 239 Hz, 1 C), 104.6 (t, $^3J_{C,F}$ = 6.9 Hz, 1 C), 91.2 (s, 1 C), 71.4 (s, 1 C), 67.3 (s, 1 C), 66.7 (s, 2 C), 46.8 (s, 1 C), 44.4 (s, 2 C), 39.1 (s, 1 C), 13.9 (s, 1 C). **NSI-HRMS** (*m/z*): $[M + H]^+$ calc. for $C_{19}H_{25}F_2N_6O_2$, 407.2002; found: 407.1989. **HPLC**: t_R = 8.60 min (97.3% purity).

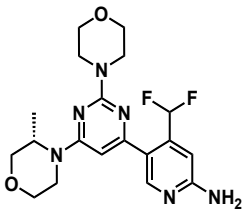

4-(Difluoromethyl)-5-{6-[(3*S*)-3-methylmorpholin-4-yl]-2-(morpholin-4-yl)pyrimidin-4-yl}pyridin-2-amine (45). Compound **45** was prepared according to general procedure 1 from intermediate **43** (73.5 mg, 246 µmol, 1.0 equiv) and boronic acid pinacol ester **49** (80.0 mg, 246 µmol, 1.0 equiv). Purification by column chromatography on silica gel (ethyl acetate / MeOH 1:0 → 100:1) gave compound **45** as a colorless solid (74.2 mg, 183 µmol, 74%). **^{1}H NMR** (400 MHz, $CDCl_3$): δ 8.31 (s, 1 H), 7.30 (t, $^2J_{H,F}$= 55 Hz, 1 H), 6.85 (s, 1 H), 6.01 (s, 1 H), 4.74 (br s, 2 H), 4.36-4.26 (m, 1 H), 4.07-3.96 (m, 1 H), 3.82-3.68 (m, 11 H), 3.57 (td, $J_{H,H}$ = 12, 3.1 Hz, 1 H), 3.24 (td, $J_{H,H}$ = 13, 3.9 Hz, 1 H), 1.30 (d, $^3J_{H,H}$ = 6.8 Hz, 3 H). **^{19}F{^{1}H} NMR** (376 MHz, $CDCl_3$): δ − 115.0 (s, 2 F). **^{13}C{^{1}H} NMR** (101 MHz, $CDCl_3$): δ 163.1 (s, 1 C), 162.5 (s, 1 C), 161.6 (s, 1 C), 159.2 (s, 1 C), 149.4 (s, 1 C), 142.6 (t, $^2J_{C,F}$ = 22 Hz, 1 C), 124.7 (s, 1 C), 111.6 (t, $^1J_{C,F}$ = 239 Hz, 1 C), 104.6 (br s, 1 C), 91.6 (s, 1 C), 71.2 (s, 1 C), 67.4-66.6 (m, 3 C), 47.2 (s, 1 C), 44.4 (s, 2 C), 39.2 (s, 1 C), 13.7 (s, 1 C). **NSI-HRMS** (*m/z*): $[M + H]^+$ calc. for $C_{19}H_{25}F_2N_6O_2$, 407.2002; found: 407.1990. **HPLC**: t_R = 7.65 min (97.2% purity).

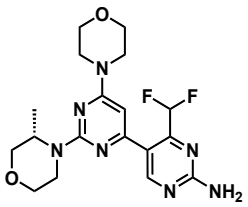

4'-(Difluoromethyl)-2-[(3*S*)-3-methylmorpholin-4-yl]-6-(morpholin-4-yl)-[4,5'-bipyrimidin]-2'-amine (46). Compound **46** was prepared according to general procedure 3 from intermediate **42** (101 mg, 338 µmol, 1.1 equiv) and compound **52** (130 mg, 306 µmol, 1.0 equiv). Purification by column chromatography on silica gel (cyclohexane / ethyl acetate 1:0 → 3:7) gave compound **46** as a colorless solid (65.8 mg, 162 µmol, 53%). **^{1}H NMR** (400 MHz, $CDCl_3$): δ 8.60 (s, 1 H), 7.13 (t, $^2J_{H,F}$ = 54 Hz, 1 H), 6.01 (s, 1 H), 5.41 (br s, 2 H), 4.72-4.62 (m, 1 H), 4.31 (dd, $^2J_{H,H}$ = 14 Hz, $^3J_{H,H}$ = 2.2 Hz, 1 H), 3.97 (dd, $J_{H,H}$ = 11, 3.4 Hz, 1 H), 3.83-3.49 (m, 11 H), 3.25 (td, $J_{H,H}$ = 13, 3.7 Hz, 1 H), 1.29 (d, $^3J_{H,H}$ = 6.8 Hz, 3 H). **^{19}F{^{1}H} NMR** (376 MHz, $CDCl_3$): δ − 119.9 (s, 2 F). **^{13}C{^{1}H} NMR** (101 MHz, $CDCl_3$): δ 163.7 (s, 1 C), 163.0 (s, 1 C), 161.0 (s, 1 C), 160.4 (br s, 2 C), 158.1 (t, $^2J_{C,F}$ = 22 Hz, 1 C), 122.6 (br s, 1 C), 110.0 (t, $^1J_{C,F}$ = 241 Hz, 1 C), 91.1 (br s, 1 C), 71.4 (s, 1 C), 67.3 (s, 1 C), 66.7 (s, 2 C), 46.8 (s, 1 C), 44.4 (s, 2 C), 39.1 (s, 1 C), 13.9 (s, 1 C). **NSI-HRMS** (*m/z*): $[M + H]^+$ calc. for $C_{18}H_{24}F_2N_7O_2$, 408.1954; found: 408.1943. **HPLC**: t_R = 7.33 min (96.2% purity).

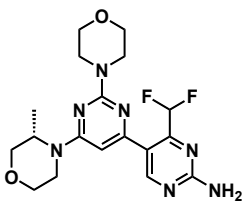

4'-(Difluoromethyl)-6-[(3*S*)-3-methylmorpholin-4-yl]-2-(morpholin-4-yl)-[4,5'-bipyrimidin]-2'-amine (47). Compound **47** was prepared according to general procedure 3 from intermediate **43** (101 mg, 338 µmol, 1.1 equiv) and compound **52** (130 mg, 306 µmol, 1.0 equiv). Purification by column chromatography on silica gel (cyclohexane / ethyl acetate 1:0 → 1:1) gave compound **47** as a colorless solid (78.2 mg, 192 µmol, 63%). **^{1}H NMR** (400 MHz, $CDCl_3$): δ 8.60 (s, 1 H), 7.11 (t, $^2J_{H,F}$ = 54 Hz, 1 H), 5.99 (s, 1 H), 5.40 (br s, 2 H), 4.35-4.25 (m, 1 H), 4.06-3.96 (m, 2 H), 3.83-3.68 (m, 10 H), 3.62-

3.52 (m, 1 H), 3.30-3.20 (m, 1 H), 1.31 (d, $^{3}J_{H,H}$ = 6.3 Hz, 3 H). **^{19}F{^{1}H} NMR** (376 MHz, $CDCl_3$): δ − 119.7 (s, 2 F). **^{13}C{^{1}H} NMR** (101 MHz, $CDCl_3$): δ 163.0 (s, 1 C), 162.9 (s, 1 C), 161.6 (s, 1 C), 160.4 (s, 1 C), 160.2 (s, 1 C), 158.1 (t, $^{2}J_{C,F}$ = 22 Hz, 1 C), 122.8 (br s, 1 C), 110.0 (t, $^{1}J_{C,F}$ = 241 Hz, 1 C), 91.5 (s, 1 C), 71.1 (s, 1 C), 67.0 (s, 2 C), 66.9 (s, 1 C), 47.3 (s, 1 C), 44.4 (s, 2 C), 39.2 (s, 1 C), 13.7 (s, 1 C). **NSI-HRMS** (*m/z*): $[M + H]^+$ calc. for $C_{18}H_{24}F_2N_7O_2$, 408.1954; found: 408.1941. **HPLC**: t_R = 6.83 min (95.6% purity).

***N*,*N*-Dimethyl-*N*'-[5-(4,4,5,5-tetramethyl-1,3,2-dioxaborolan-2-yl)-4-(trifluoromethyl)pyridin-2-yl]methanimidamide (48).** Compound **48** was prepared according to the literature.[9]

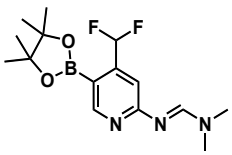

***N*'-[4-(Difluoromethyl)-5-(4,4,5,5-tetramethyl-1,3,2-dioxaborolan-2-yl)pyridin-2-yl]-*N*,*N*-dimethylmethanimidamide (49).** Compound **49** was prepared according to the literature.[17]

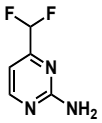

4-(Difluoromethyl)pyrimidin-2-amine (50). *Step 1.* To a solution of ethyl vinyl ether (4.00 mL, 41.8 mmol, 1.0 equiv) in a mixture of pyridine (4.10 mL, 50.7 mmol, 1.2 equiv) and dichloromethane (40 mL) at − 70 °C in a dry ice / isopropanol bath, a solution of 2,2-difluoroacetic anhydride (5.90 mL, 50.1 mmol, 1.2 equiv) in dichloromethane (5 mL) was added dropwise. The resulting solution was allowed to warm up to room temperature overnight. The mixture was then washed with deionized H_2O, the organic layer was dried over anhydrous Na_2SO_4, filtered and the solvent was evaporated under reduced pressure to afford an orange oil. *Step 2.* A solution of guanidine·HCl (4.80 g, 50.2 mmol, 1.2

equiv) in ethanol (20 mL) was stirred at room temperature for 1 hour. To this solution, NaOH pellets (2.00 g, 50.0 mmol, 1.2 equiv) were added in one portion and the suspension was stirred at room temperature overnight. The above oil was diluted with dichloromethane (20 mL) and added drop wise over 1 hour to the guanidine suspension. The resulting suspension was stirred at room temperature for 2 hours. Dichloromethane was evaporated under reduced pressure. Deionized H_2O (25 mL) was added to the residue and the resulting mixture was stirred vigorously for 2 hours and was then allowed to stand at room temperature overnight. The solid was filtered off, washed with deionized H_2O (2 x) and heptanes (1 x) and dried under reduced pressure. The desired product **50** was obtained as a colorless solid (3.94 g, 27.2 mmol, 65%). **^{1}H NMR** (400 MHz, $(CD_3)_2SO$): δ 8.43 (d, $^2J_{H,H}$ = 4.8 Hz, 1 H), 7.02 (br s, 2 H), 6.76 (d, $^2J_{H,H}$ = 5.2 Hz, 1 H), 6.67 (t, $^2J_{H,F}$ = 55 Hz, 1 H). **^{19}F{^{1}H} NMR** (376 MHz, $CDCl_3$): δ − 120.5 (s, 2 F). **^{13}C{^{1}H} NMR** (101 MHz, $CD_3)_2SO$): δ 163.5 (br s, 1 C), 160.4 (s, 1 C), 160.3 (t, $^2J_{C,F}$ = 25 Hz, 1 C), 112.6 (t, $^1J_{C,F}$ = 240 Hz, 1 C), 105.0 (t, $^3J_{C,F}$ = 4.0 Hz, 1 C).

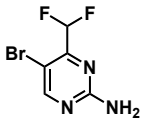

5-Bromo-4-(difluoromethyl)pyrimidin-2-amine (51). To a solution of compound **50** (3.00 g, 20.7 mmol, 1.0 equiv) in tetrahydrofuran (90 mL) at 0 °C, *N*-bromosuccinimide (3.86 g, 21.7 mmol, 1.0 equiv.) was added portion wise. The reaction mixture was allowed to warm up to room temperature overnight. Then, the solvent was evaporated under reduced pressure. The residue was washed with deionized H_2O (2 x 5 mL), cold ethyl acetate (1 x 5 mL) and dried under reduced pressure. The desired product **51** was obtained as a yellowish solid, which was used in the next step without further purification (4.54 g, 20.3 mmol, 98% yield). **^{1}H NMR** (400 MHz, $(CD_3)_2SO$): δ 8.50 (s, 1 H), 7.30 (br s, 2 H), 6.87 (t, $^2J_{H,F}$ = 53 Hz, 1 H). **^{19}F{^{1}H} NMR** (376 MHz, $(CD_3)_2SO$): δ − 121.4 (s, 2 F). **^{13}C{^{1}H} NMR** (101 MHz, $(CD_3)_2SO$): δ 162.1 (s, 1 C), 161.6 (s, 1 C), 156.1 (t, $^2J_{C,F}$ = 23 Hz, 1 C), 112.0 (t, $^1J_{C,F}$ = 241 Hz, 1 C), 101.7 (s, 1 C).

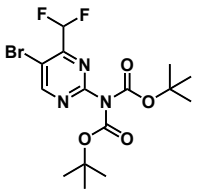

***tert*-Butyl *N*-[5-bromo-4-(difluoromethyl)pyrimidin-2-yl]-*N*-[(*tert*-butoxy)carbonyl]carbamate (52).** To a solution of compound **51** (4.35 g, 19.4 mmol, 1.0 equiv) and 4-(dimethylamino)pyridine (480 mg, 3.92 mmol, 0.20 equiv.) were dissolved in tetrahydrofuran (50 mL) at 0 °C, *N*,*N*-Diisopropylethylamine (7.50 mL, 42.1 mmol, 2.2 equiv) and di-*tert*-butyl dicarbonate (9.33 g, 42.7 mmol, 2.2 equiv) were added. The resulting solution was allowed to warm up to room temperature overnight. The solvent was evaporated under reduced pressure. The crude product was purified by column chromatography on silica gel (cyclohexane / ethyl acetate 9:1 → 4:1) to afford the desired product **52** as a colorless solid (7.00 g, 16.5 mmol, 85% yield). **^{1}H NMR** (400 MHz, $CDCl_3$): δ 8.92 (s, 1 H), 6.73 (t, $^{2}J_{H,F}$ = 53 Hz, 1 H), 1.47 (s, 18 H). **^{19}F{^{1}H} NMR** (376 MHz, $CDCl_3$): δ − 120.4 (s, 2 F). **^{13}C{^{1}H} NMR** (101 MHz, $CDCl_3$): δ 162.6 (s, 2 C), 158.1 (t, $^{2}J_{C,F}$ = 25 Hz, 1 C), 157.5 (s, 1 C), 150.2 (s, 1 C), 114.5 (s, 1 C), 111.8 (t, $^{1}J_{C,F}$ = 244 Hz, 1 C), 84.4 (s, 2 C), 27.9 (s, 6 C).

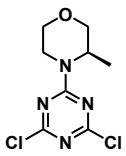

2,4-Dichloro-6-[(3*R*)-3-methylmorpholin-4-yl]-1,3,5-triazine (53). To a solution of cyanuric chloride (9.00 g, 48.8 mmol, 1.0 equiv) in dichloromethane (200 mL), a solution of *N*,*N*-diisopropylethylamine (8.50 mL, 48.9 mmol, 1.0 equiv) and (*R*)-3-methylmorpholine (4.90 g, 48.9 mmol, 1.0 equiv) in dichlomethane (60 mL) was slowly added at − 50 °C. The mixture was stirred at − 50 °C for 2 hours. Aqueous saturated $NaHSO_4$-solution (200 mL) was added and the resulting mixture was allowed to warm up to room temperature. The organic layer was separated, washed with aqueous saturated $NaHSO_4$-solution (100 mL), dried over anhydrous Na_2SO_4, filtered and the solvent was evaporated under reduced pressure. The product was recrystallized from dichloromethane / heptanes to afford **53** a colorless solid (9.30 g, 37.3 mmol, 76%). **^{1}H NMR** (400 MHz, $(CD_3)_2SO$): δ 4.59-4.50 (m, 1 H), 4.24-4.15 (m, 1 H), 3.91 (dd, $J_{H,H}$ = 11, 3.5 Hz,

1 H), 3.69 (d, $J_{H,H}$ = 12 Hz, 1 H), 3.56 (dd, $J_{H,H}$ = 12, 3.1 Hz, 1 H), 3.46-325 (m, 2 H), 1.26 (d, $J_{H,H}$ = 6.9 Hz, 3 H). **^{13}C{^{1}H} NMR** (101 MHz, $CDCl_3$): δ 170.6 (s, 1 C), 170.4 (s, 1 C), 164.0 (s, 1 C), 70.7 (s, 1 C), 66.6 (s, 1 C), 47.8 (s, 1 C), 39.6 (s, 1 C), 14.8 (s, 1 C).

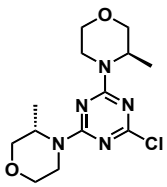

2-Chloro-4-[(3*R*)-3-methylmorpholin-4-yl]-6-[(3*S*)-3-methylmorpholin-4-yl]-1,3,5-triazine (54).

To a solution of (*S*)-3-methylmorpholine (128 mg, 1.27 mmol, 1.1 equiv) and *N*,*N*-diisopropylethylamine (500 µl, 2.87 mmol, 2.4 equiv) in dichloromethane (3 mL), a solution of cyanuric chloride (300 mg, 1.20 mmol, 1.0 equiv) in dichloromethane (2 mL) was added dropwise at 0 °C in an ice bath. The resulting reaction mixture was stirred overnight, while it was allowed to warm up to room temperature. Additional dichloromethane was added and the organic layer was washed with an aqueous saturated $NaHSO_4$-solution (2 x). The organic layer was dried over anhydrous Na_2SO_4, filtered and the solvent was evaporated under reduced pressure. The crude product was purified by column chromatography on silica gel (cyclohexane / ethyl acetate 1:0 → 7:3) to afford compound **54** as a colorless solid (371 mg, 1.18 mmol, 99%). **^{1}H NMR** (400 MHz, $CDCl_3$): δ 4.74-4.56 (m, 2 H), 4.39-4.22 (m, 2 H), 3.94 (dd, $J_{H,H}$ = 12, 3.7 Hz, 2 H), 3.73 (d, $J_{H,H}$ = 12 Hz, 2 H), 3.63 (dd, $J_{H,H}$ = 12, 3.2 Hz, 2 H), 3.48 (td, $J_{H,H}$ = 12, 3.0 Hz, 2 H), 3.24 (td, $J_{H,H}$ = 13, 3.8 Hz, 2 H), 1.30 (d, $^{3}J_{H,H}$ = 6.9 Hz, 6 H). **^{13}C{^{1}H} NMR** (101 MHz, $CDCl_3$): δ 169.7 (s, 1 C), 164.4 (s, 2 C), 71.0 (s, 2 C), 66.9 (s, 2 C), 46.8 (s, 2 C), 38.9 (s, 2 C), 14.7 (br s, 1 C), 14.3 (br s, 1 C). **MALDI-MS**: *m/z* = 313.7 ($[M + H]^+$).

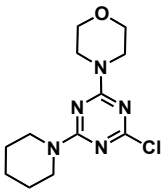

2-Chloro-4-(morpholin-4-yl)-6-(piperidin-1-yl)-1,3,5-triazine (55). 4-(4,6-Dichloro-1,3,5-triazin-2-yl)morpholine (**23**, 500 mg, 2.13 mmol, 1.0 equiv), piperidine (230 µl, 2.34 mmol, 1.1 equiv) and *N*,*N*-diisopropylethylamine (810 µl, 4.68 mmol, 2.2 equiv) were dissolved in ethanol (10 mL) and the resulting mixture was stirred at room temperature overnight. The solvent was then evaporated under reduced pressure and the crude product was purified by column chromatography on silica gel gel (cyclohexane / ethyl acetate 1:0 → 9:1) to afford compound **55** as a colorless solid (547 mg, 1.93 mmol, 91%). The spectroscopic data are consistent with previous literature reports.[31]

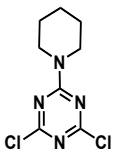

2,4-Dichloro-6-(piperidin-1-yl)-1,3,5-triazine (56). To a solution of cyanuric chloride (500 mg, 2.71 mmol, 1.0 equiv) in dichloromethane (12 mL) a solution of piperidine (268 µl, 2.71 mmol, 1.0 equiv) and *N*,*N*-diisopropylethylamine (471 µl, 2.71 mmol, 1.0 equiv) in dichloromethane (4 mL) was slowly added at − 77 °C (dry ice / *iso*propanol bath). The resulting reaction mixture was stirred overnight, while it was allowed to warm up to room temperature. Additional dichloromethane (10 mL) was added and the organic layer was washed with an aqueous saturated $NaHSO_4$-solution (2 x). The organic layer was dried over anhydrous Na_2SO_4, filtered and the solvent was evaporated under reduced pressure. The desired product **56** was isolated as a colorless solid and used in the next step without further purification (567 mg, 2.44 mmol, 90%). The spectroscopic data are consistent with previous literature reports.[32]

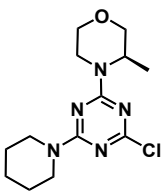

2-Chloro-4-[(3*R*)-3-methylmorpholin-4-yl]-6-(piperidin-1-yl)-1,3,5-triazine (57).

2,4-Dichloro-6-(piperidin-1-yl)-1,3,5-triazine (**56**, 180 mg, 772 µmol, 1.0 equiv), (*R*)-3-methylmorpholine (78.1 mg, 772 µmol, 1.0 equiv) and *N*,*N*-diisopropylethylamine (283 µl, 1.62 mmol, 2.1 equiv) were mixed in 1,4-dioxane / dichloromethane (4:1 mL) and the resulting suspension was stirred at room temperature overnight. The solvent was then evaporated under reduced pressure and the crude product was purified by column chromatography on silica gel gel (cyclohexane / ethyl acetate 1:0 → 19:1) to afford compound **57** as a colorless solid (218 mg, 732 µmol, 95%). **^{1}H NMR** (400 MHz, $CDCl_3$): δ 4.72-4.60 (m, 1 H), 4.36-4.26 (m, 1 H), 3.92 (dd, $J_{H,H}$ = 11, 3.4 Hz, 1 H), 3.79-3.65 (m, 5 H), 3.63 (dd, $J_{H,H}$ = 12, 3.0 Hz, 1 H), 3.47 (td, $J_{H,H}$ = 12, 2.8 Hz, 1 H), 3.23 (td, $J_{H,H}$ = 13, 3.8 Hz, 1 H), 1.71-1.52 (m, 6 H), 1.29 (d, $^{3}J_{H,H}$ = 6.9 Hz, 3 H). **^{13}C{^{1}H} NMR** (101 MHz, $CDCl_3$): δ 169.7 (s, 1 C), 164.4 (s, 1 C), 164.2 (s, 1 C), 71.0 (s, 1 C), 67.0 (s, 1 C), 46.7 (s, 1 C), 44.6 (br s, 2 C), 38.9 (s, 1 C), 25.9 (br s, 1 C), 25.7 (br s, 1 C), 24.7 (s, 1 C), 14.4 (br s, 1 C). **MALDI-MS**: *m/z* = 298.4 ($[M + H]^+$).

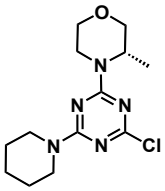

2-Chloro-4-[(3*S*)-3-methylmorpholin-4-yl]-6-(piperidin-1-yl)-1,3,5-triazine (58). Compound **58** was prepared in the same manner than its enantiomer described above from 2,4-dichloro-6-(piperidin-1-yl)-1,3,5-triazine (**56**) and (*S*)-3-methylmorpholine in 98% yield. The spectroscopic data are in agreement with those reported for the (*R*)-enantiomer **57**.

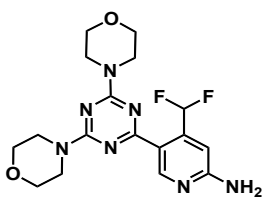

5-[4,6-Bis(morpholin-4-yl)-1,3,5-triazin-2-yl]-4-(difluoromethyl)pyridin-2-amine (59). Compound **59** was prepared according to the literature.[17]

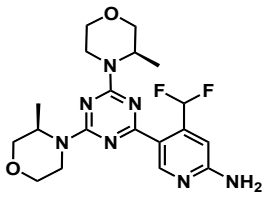

5-{4,6-Bis[(3*R*)-3-methylmorpholin-4-yl]-1,3,5-triazin-2-yl}-4-(difluoromethyl)pyridin-2-amine (60). Compound **60** was prepared according to general procedure 1 from intermediate **9** (250 mg, 786 µmol, 1.0 equiv) and boronic acid pinacol ester **49** (285 mg, 876 µmol, 1.1 equiv). Purification by column chromatography on silica gel (cyclohexane / ethyl acetate 1:0 → 2:3) gave compound **60** as a colorless solid (327 mg, 776 µmol, 98%). **^{1}H NMR** (400 MHz, $CDCl_3$): δ 8.97 (s, 1 H), 7.70 (t, $^2J_{H,F}$ = 55 Hz, 1 H), 6.86 (s, 1 H), 5.48 (br s, 2 H), 4.77-4.66 (m, 2 H), 4.45-4.34 (m, 2 H), 3.98 (dd, $J_{H,H}$ = 11, 3.7 Hz, 2 H), 3.77 (d, $J_{H,H}$ = 11 Hz, 2 H), 3.67 (dd, $J_{H,H}$ = 12, 3.2 Hz, 2 H), 3.52 (td, $J_{H,H}$ = 12, 3.0 Hz, 2 H), 3.27 (td, $J_{H,H}$ = 13, 3.8 Hz, 2 H), 1.33 (d, $^3J_{H,H}$ = 6.8 Hz, 6 H). **^{19}F{^{1}H} NMR** (376 MHz, $CDCl_3$): δ − 114.4-(− 118.1) (m, 2 F). **^{13}C{^{1}H} NMR** (101 MHz, $CDCl_3$): δ 169.3 (s, 1 C), 164.5 (s, 2 C), 160.2 (s, 1 C), 152.5 (s, 1 C), 143.7 (t, $^2J_{C,F}$ = 22 Hz, 1 C), 121.8-121.5 (m, 1 C), 111.5 (t, $^1J_{C,F}$ = 239 Hz, 1 C), 104.1 (t, $^3J_{C,F}$ = 7.9 Hz, 1 C), 71.2 (s, 2 C), 67.1 (s, 2 C), 46.5 (s, 2 C), 38.7 (s, 2 C), 14.4 (s, 2 C). **MALDI-MS**: *m/z* = 421.7 ([M + H]$^+$). **HPLC**: t_R = 8.28 min (99.2% purity).

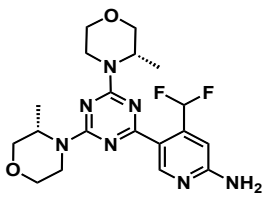

5-{4,6-Bis[(3*S*)-3-methylmorpholin-4-yl]-1,3,5-triazin-2-yl}-4-(difluoromethyl)pyridin-2-amine (61). Compound **61** was prepared in the same manner than its enantiomer described above from intermediate **10** and boronic acid pinacol ester **49** in 79% yield. The spectroscopic data are in agreement with those reported for the (*R*,*R*)-enantiomer **60**. **HPLC**: t_R = 6.39 min (95.2% purity).

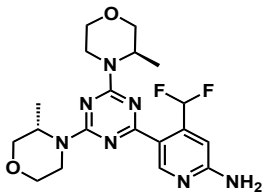

4-(Difluoromethyl)-5-{4-[(3*R*)-3-methylmorpholin-4-yl]-6-[(3*S*)-3-methylmorpholin-4-yl]-1,3,5-triazin-2-yl}pyridin-2-amine (**62**). Compound **62** was prepared according to general procedure 1 from intermediate **54** (271 mg, 864 µmol, 1.0 equiv) and boronic acid pinacol ester **49** (309 mg, 950 µmol, 1.1 equiv). Purification by column chromatography on silica gel (cyclohexane / ethyl acetate 1:0 → 2:3) gave compound **62** as a colorless solid (152 mg, 361 µmol, 42%). ^{1}H NMR (400 MHz, $CDCl_3$): δ 9.04 (s, 1 H), 7.69 (t, $^{2}J_{H,F}$ = 55 Hz, 1 H), 6.84 (s, 1 H), 4.83 (br s, 2 H), 4.78-4.68 (m, 2 H), 4.45-4.33 (m, 2 H), 3.98 (dd, $J_{H,H}$ = 11, 3.2 Hz, 2 H), 3.77 (d, $J_{H,H}$ = 11 Hz, 2 H), 3.68 (dd, $J_{H,H}$ = 11, 2.9 Hz, 2 H), 3.53 (td, $J_{H,H}$ = 12, 2.7 Hz, 2 H), 3.33-3.22 (m, 2 H), 1.32 (d, $^{3}J_{H,H}$ = 6.9 Hz, 6 H). **^{19}F{^{1}H} NMR** (376 MHz, $CDCl_3$): δ − 116.3 (s, 2 F). **^{13}C{^{1}H} NMR** (101 MHz, $CDCl_3$): δ 169.3 (s, 1 C), 164.5 (s, 2 C), 160.2 (s, 1 C), 152.5 (s, 1 C), 143.7 (t, $^{2}J_{C,F}$ = 22 Hz, 1 C), 121.6 (t, $^{3}J_{C,F}$ = 4.8 Hz, 1 C), 111.5 (t, $^{1}J_{C,F}$ = 239 Hz, 1 C), 104.1 (t, $^{3}J_{C,F}$ = 7.9 Hz, 1 C), 71.2 (s, 2 C), 67.1 (s, 2 C), 46.5 (s, 2 C), 38.7 (s, 2 C), 14.4 (s, 2 C). **MALDI-MS**: *m/z* = 422.1 ([M + H]$^{+}$). **HPLC**: t_R = 8.39 min (99.5% purity).

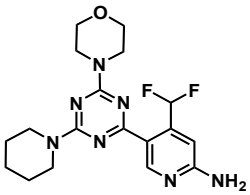

4-(Difluoromethyl)-5-[4-(morpholin-4-yl)-6-(piperidin-1-yl)-1,3,5-triazin-2-yl]pyridin-2-amine (63). Compound **63** was prepared according to general procedure 1 from intermediate **55** (250 mg, 881 µmol, 1.0 equiv) and boronic acid pinacol ester **49** (301 mg, 926 µmol, 1.1 equiv). Purification by column chromatography on silica gel (cyclohexane / ethyl acetate 1:0 → 2:3) gave compound **63** as a colorless solid (107 mg, 273 µmol, 31%). **^{1}H NMR** (400 MHz, $CDCl_3$): δ 9.02 (s, 1 H), 7.69 (t, $^{2}J_{H,F}$ = 55 Hz, 1 H), 6.83 (s, 1 H), 4.83 (br s, 2 H), 3.87-3.71 (m, 12 H), 1.73-1.64 (m, 2 H), 1.64-1.55 (m, 4 H). **^{19}F{^{1}H} NMR** (376 MHz, $CDCl_3$): δ − 116.2 (s, 2 F). **^{13}C{^{1}H} NMR** (101 MHz,

$CDCl_3$): δ 169.2 (s, 1 C), 165.0 (s, 1 C), 164.4 (s, 1 C), 160.1 (s, 1 C), 152.3 (s, 1 C), 143.7 (t, $^2J_{C,F}$ = 22 Hz, 1 C), 122.0 (t, $^3J_{C,F}$ = 5.0 Hz, 1 C), 111.5 (t, $^1J_{C,F}$ = 239 Hz, 1 C), 104.1 (t, $^3J_{C,F}$ = 7.8 Hz, 1 C), 67.0 (s, 2 C), 44.4 (s, 1 C), 43.7 (s, 2 C), 25.9 (s, 2 C), 25.0 (s, 2 C). **MALDI-MS**: *m/z* = 392.5 ($[M + H]^+$). **HPLC**: t_R = 9.20 min (96.7% purity).

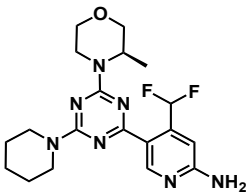

4-(Difluoromethyl)-5-{4-[(3*R*)-3-methylmorpholin-4-yl]-6-(piperidin-1-yl)-1,3,5-triazin-2-yl}pyridin-2-amine (64). Compound **64** was prepared according to general procedure 1 from intermediate **57** (139 mg, 466 µmol, 1.0 equiv) and boronic acid pinacol ester **49** (152 mg, 467 µmol, 1.0 equiv). Purification by column chromatography on silica gel (cyclohexane / ethyl acetate 1:0 → 2:3) gave compound **64** as a colorless solid (78.5 mg, 194 µmol, 41%). **^{1}H NMR** (400 MHz, $CDCl_3$): δ 9.03 (s, 1 H), 7.71 (t, $^2J_{H,F}$ = 55 Hz, 1 H), 6.83 (s, 1 H), 4.82 (br s, 2 H), 4.78-4.69 (m, 1 H), 4.45-4.36 (m, 1 H), 3.97 (dd, $J_{H,H}$ = 11, 3.4 Hz, 1 H), 3.86-3.72 (m, 5 H), 3.68 (dd, $J_{H,H}$ = 11, 3.0 Hz, 1 H), 3.53 (td, $J_{H,H}$ = 12, 2.9 Hz, 1 H), 3.26 (td, $J_{H,H}$ = 13, 3.7 Hz, 1 H), 1.73-1.54 8m, 6 H), 1.32 (d, $^3J_{H,H}$ = 6.8 Hz, 3 H). **^{19}F{^{1}H} NMR** (376 MHz, $CDCl_3$): δ − 115.3-(− 117.5) (m, 2 F). **^{13}C{^{1}H} NMR** (101 MHz, $CDCl_3$): δ 169.2 (s, 1 C), 164.6 (s, 1 C), 164.4 (s, 1 C), 160.1 (s, 1 C), 152.3 (s, 1 C), 143.6 (t, $^2J_{C,F}$ = 22 Hz, 1 C), 122.0 (t, $^3J_{C,F}$ = 4.9 Hz, 1 C), 111.5 (t, $^1J_{C,F}$ = 239 Hz, 1 C), 104.1 (t, $^3J_{C,F}$ = 7.8 Hz, 1 C), 71.2 (s, 1 C), 67.2 (s, 1 C), 46.4 (s, 1 C), 44.4 (br s, 2 C), 38.6 (s, 1 C), 25.9 (br s, 2 C), 25.0 (s, 1 C), 14.3 (s, 1 C). **MALDI-MS**: *m/z* = 406.3 ($[M + H]^+$). **HPLC**: t_R = 9.74 min (98.9% purity).

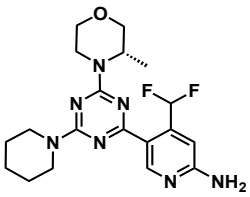

4-(Difluoromethyl)-5-{4-[(3*S*)-3-methylmorpholin-4-yl]-6-(piperidin-1-yl)-1,3,5-triazin-2-yl}pyridin-2-amine (65). Compound **65** was prepared in the same manner than its enantiomer described above from intermediate **58** and boronic acid pinacol ester **49** in 46% yield. The spectroscopic data are in agreement with those reported for the (*R*)-enantiomer **64**. **HPLC**: t_R = 9.75 min (99.0% purity).

Cellular PI3K and mTOR signaling

Protein phosphorylation was detected as follows: pSer473 of PKB/Akt with rabbit polyclonal antibody from Cell Signaling Technology (CST), #4058); pSer235/236 on the ribosomal protein S6 (pS6RP) with rabbit monoclonal antibody from CST, #4856) by In-Cell Western assays, where $2x10^4$ A2058 or $1.6x10^4$ SKOV3 cells/well in 96-well plates were plated (Cell Carrier, Perkin Elmer) for 24 h (37°C, 5%CO_2). Inhibitors were incubated for 1 h, before cells were fixed (4% PFA in PBS for 30 min at RT), blocked (1% BSA/0.1% Triton X-100/5% goat serum in PBS for 30 min, RT), and stained with the above primary antibodies (1:500). Tubulin was detected with mouse anti-α-tubulin (1:2000, Sigma #T9026). Secondary antibodies were IRDye680-conjugated goat anti-mouse, and IRDye800-conjugated goat anti-rabbit antibodies from LICOR (# 926-68070 and # 926-32211, at 1:500). Fluorescence was measured on an Odyssey CLx infrared imaging scanner (LICOR). Percentage of remaining phospho-substrate signals were calculated in relation to cellular tubulin. Further details and calculations are explained in Ref. 9. Alternatively, phosphoprotein levels were assessed in A2058 cell lysates using the MSD platform in combination with the Akt Signaling Panel II Whole Cell Lysate Kit according to the manufacturer's instructions (MSD, Maryland US).

Determination of inhibitor dissociation constants

Dissociation constants of compounds (K_i) for p110α and mTOR were determined by LanthaScreen technology (Life Technologies) as described in detail in Ref. 9. and Ref. 10, respectively. Briefly, the AlexaFluor647-labeled Kinase Tracer314 (#PV6087) was used for p110α with a determined K_d of 2.2 nM at 20 nM, and for mTOR with a K_d of 19 nM used at a final concentration of 10 nM. While recombinant p110α was N-terminally $(His)_6$-tagged, and combined with a biotinylated anti-$(His)_6$-tag antibody (2 nM, #PV6089) and LanthaScreen Eu-Steptavidin (2 nM, #PV5899); truncated mTOR (amino acids 1360-2549; #PR8683B) fused to the C-terminus of GST was detected with a LanthaScreen Eu-labelled anti-GST antibody (2 nM, #PV5594). The p110α assay buffer was composed of 50 mM HEPES pH 7.5, 10 mM $MgCl_2$, 1 mM EGTA, and 0.01% (v/v) Brij-35, and the mTOR assay buffer contained 50 mM HEPES; 5 mM $MgCl_2$; 1mM EGTA; 0.01% Pluronic F-127. Further details and calculations are described in Ref. 9.

Wortmannin Competition Assay

Wortmannin-binding to PI3K[19,23] was measured as described earlier.[20] Briefly, recombinant p110α/p85α protein complex (PV4789 from Life Technologies; stock 0.37 mg/mL, 1.7 µM) was dissolved to 50 nM in HEPES reaction buffer (50 mM HEPES, 10 mM $MgCl_2$, 0.01% Brij-35, pH 7.4), before inhibitors were added (5 µM, 60 min., 37°C). Wortmannin was subsequently supplemented to a final concentration of 200 nM, followed by incubation for 20 min. on ice. After SDS-PAGE and immuno-blotting (to PVDF), wortmannin covalently bound to p110α was detected using rabbit anti-wortmannin antibodies.[20] PI3K p110α protein was detected with monoclonal mouse anti-p110α (clone U3A, kindly donated by A. Klippel), and p85α with our rabbit anti-p85α antibodies (H-96-Sph1).

Purification of PI3Kα protein for structural studies

PI3Kα (ΔABD-LBS p110α 105-1048) was expressed by recombinant baculovirus in Sf9 cells, purified, and initially crystalized as previously published.[24] In brief, p110α was produced in *Spodoptera frugiperda* (Sf9) cells by infecting 1 L of cells at a density of 1.5 x 10^6 cells/mL with baculovirus

encoding the kinase. After 65 hours of infection at 27° C cells were harvested and washed with phosphate-buffered saline (PBS). The p110α construct contained an N-terminal 2X Strep Tag followed by a 10X histidine tag and Tobacco Etch Virus (TEV) protease cleave site. Sf9 pellets were lysed in 50 mM Tris pH 8.0, 250 mm NaCl, 0.25 mM TCEP, 20 mM imidazole, protease inhibitor (Protease Inhibitor Cocktail Set III, Sigma) using sonication, Triton X-100 was added to 0.5% (v/v) and lysed material was centrifuged at 20000 x g (Beckman J2-21, Beckman JA-20 rotor). Supernatant was passed through a 5 μm filter and onto a HisTrap FF Crude column pre-equilibrated in 50 mM Tris pH 8.0, 250 mm NaCl, 0.25 mM TCEP, and 20 mM imidazole. Protein was eluted from the column using 50 mM Tris pH 8.0, 200 mm NaCl, 0.25 mM TCEP and 200 mM imidazole. Eluted protein was passed through a 5.0 mL StepTrapHP column pre-equilibrated in 50 mM Tris pH 8.0, 250 mm NaCl, 0.25 mM TCEP, and 20 mM imidazole. The column was washed with 5.0 mL of 50 mM Tris pH 8.0, 200 mm NaCl, 0.25 mM TCEP, and 40 mM imidazole, and 5.0 mL of TEV protease (0.01 mg/L) was added to the column for overnight cleavage at 4 °C. The protein was eluted with 7.0 mL of 50 mM Tris pH 8.0, 200 mm NaCl, 0.25 mM TCEP, and 40 mM imidazole and concentrated using an Amicon 50-kDa MWCO concentrator (MilliporeSigma) to 1.0 mL. The protein was loaded onto a Superdex 200 10/300 GL Increase (GE Healthcare) in 50 mM Tris PH 8.0, 100 mM NaCl, 2% Ethylene Glycol and 1 mM TCEP, and protein from a single peak was collected. Protein was concentrated using an Amicon 50-kDa MWCO concentrator to 6.5 mg/mL, flash frozen as small aliquots in liquid nitrogen and stored at -80 °C.

Crystallography

Initial *apo* p110α crystallography hits were obtained from a grid of 1 μL hanging drops containing 0.5 μL protein at 5.8 mg/mL (in 50 mM Tris pH 8.0, 100 mM NaCl, 2% EG, 1mM TCEP pH 7.5) mixed 1:1 with 0.5 μL reservoir (PEG6000 6-12%, 0.6 M Sodium Formate, 0.1 M CHES pH 9.1-9.7, 5 mM TCEP pH 7.5) at a temperature of 18 °C. Crystals collected for diffraction were obtained from 1 uL hanging drop containing 0.5 μL protein at 5.8 mg/mL with a two-fold molar excess of AFO-30 mixed with 0.4 μL reservoir (8% PEG6000, 0.6M Na Formate, 0.1M CHES pH 9.5, 5mM TCEP pH 7.5) and

0.1 μL of 1/1000 diluted micro-seeds crushed from a drop of the original *apo* crystals. Crystals were flash-frozen in liquid nitrogen after transferring to 1 μL reservoir solution containing 25% (v/v) glycerol as cryoprotectant and then stored in liquid nitrogen.

Diffraction data for the PI3K crystals were collected at 100 K at beamline BL14-1 of the Stanford Synchrotron Radiation Lightsource (SSRL). Data were processed using XDS.[25] Phases were initially obtained by molecular replacement using Phaser,[26] with the structure of truncated PI3Kα (PDB ID: 4TUU[24]). Iterative model building and refinement were performed in COOT[27] and phenix.refine,[28] with a final Rwork=24.2 and Rfree=28.7 for the PI3Kα structure bound to PQR530. Refinement was carried out with rigid body refinement followed by Translation/Libration/Screw B-factor and xyz refinement. The final model was verified in Molprobity for the absence of both Ramachandran and Rotamer outliers.[29] Data collection and refinement statistics are shown in Supporting Information Table S3.

Structure modelling & determination

The X-ray structure of PQR309 (**1**) in PI3Kγ (PDB code 5OQ4, 2.7 Å) was used as starting point. The morpholine of PQR309 (**1**) pointing into the hinge region of PI3Kγ was substituted at the C3-position with a methyl group in (*S*)- and (*R*)-configuration. Energy minimization calculations for the resulting PI3Kγ-ligand complexes were carried out. All the four possible orientations were analyzed and superimposed. For mTOR kinase, the 3.6 Å resolution X-ray structure of PI103 in mTOR (PDB code 4JT6) was exploited as a starting point. PI103 was substituted for PQR530 (**6**) and its (*R*)-enantiomer (**66**). In analogy to PI3K, the two possible orientations of PQR530 (**6**) and **66** were analyzed and superimposed. Further measurements and figures were generated in Maestro11.1 as described in Ref. 17.

Kinome profiling

The inhibitory capacity and selectivity of compound was determined using the ScanMax platform provided by DiscoverX.[16] In short binding of immobilized ligand to DNA-tagged kinases was competed with 10 μM compound. The amount of kinase bound to the immobilized ligand was measured by

quantitative PCR of the respective DNA tags and is given as percentage of control. Binding constants of compounds for kinases of interest were determined by competing the immobilized ligand kinase interactions with an 11-point 3-fold serial dilution of compound starting from 30 μM and subsequent quantitative PCR of DNA tags. Binding constants were calculated by a standard dose-response curve using the Hill equation (with Hill Slope set to -1):

Response = Background + (Signal - Background)/(1 + 10^([lg Kd - lg dose] * HillSlope))

Selectivity scores[30] were calculated as

S = Number of hits / Number of tested kinases (excluding mutant variants),

where S35, S10, S1 were calculated using %Ctrl as a potency threshold (35, 10, 1%); for example

S(35) = (number of non-mutant kinases with %Ctrl <35)/(number of non-mutant kinases tested).

Viability studies – 66 cancer cell line panel

The NTRC Oncolines 66 cell lines were exposed for 72 h to 9-point 3.16-fold serial dilutions of PQR530 (**6**) as described in Ref. 9. and Ref. 10. The IC_{50}s were calculated by non-linear regression using IDBS XLfit 5. The percentage growth after 72h (%-growth) was normalized as follows:

$$100\% * (\text{luminescence}_{t=72h} / \text{luminescence}_{\text{untreated},t=72h}).$$

This was fitted to a 4-parameter logistics curve:

$$\%\text{-growth} = \text{bottom} + (\text{top} - \text{bottom}) / (1 + 10^{[(\text{Log } IC_{50} - \text{Log } x) * \text{HillSlope}]}),$$

where bottom and top are the asymptotic minimum and maximum cell growth that the compound allows in that assay.

The LD_{50}, the concentration at which 50% of cells die, is the concentration where:

$$\text{luminescence}_{t = 72h} = ½ \text{ x luminescence}_{t = 0h}$$

The GI_{50}, the concentration of 50% growth inhibition, is the concentration where cell growth is half maximum. This is concentration associated with the signal:

$$((\text{luminescence}_{\text{untreated},t=72h} - \text{luminescence}_{t=0}) /2) + \text{luminescence}_{t=0}$$

Cell proliferation assays

A2058 and SKOV3 cell proliferation assays were performed as described in Ref. 9. Briefly, cells were seeded in 95 µl complete DMEM to 96-well plates (Cell Carrier; Perkin Elmer) 24 h before inhibitor treatment (5 to 0.02 µM for 72 hours). Fixation was achieved by the addition of 65 µl 10% paraformaldehyde (PFA) in PBS for 30 min (RT). Hoechst33324 staining followed by addition of 1:10 volume of 1% BSA/1% Triton X-100, 10mg/mL Hoechst33324 in PBS (30 min, RT). Fluorescent images were acquired with an Operetta high content system (Perkin Elmer). 35 fields of view were acquired per well [20x WD objective, with a Hoechst33324 compatible filter combination (excitation 380/20 nm, 405 nm dichroic mirror, emission 445/70 nm)].

Formulation of compounds for *in vivo* experiments.

Compound **6** (6.25 mg) were dissolved in DMSO (0.25 mL) by vortexing and sonication. After the addition of 2.25 mL 20% HP-β-CD (hydroxypropyl-β-cyclodextrin/water) the mixture was vortexed and sonicated to get 2.5 mL dosing solution. Formulations were homogenous at the time of application.

OVCAR-3 xenograft mouse tumor model

OVCAR-3 cell culture: cells were cultured as monolayer in DMEM medium supplemented with 10% fetal bovine serum at 37ºC5% CO_2. Cells were passaged by trypsin-EDTA treatment, and harvested in the exponential growth phase tumor inoculation.

Tumor inoculation and group assignments: each mouse (female BALB/c nude; age: 8-9 weeks) was inoculated subcutaneously with 5×10^6 cells (in 0.1 mL PBS) into the right flank. At treatment start mean tumor size was ca. 157 mm^3, body weight and tumor volume were assessed, and randomized groups using a randomized block design based on tumor volumes were established. Tumor cell inoculation is depicted as day 0.

Data collection and termination: Animals were monitored daily for mobility, visual estimation of food and water consumption, eye/hair matting, morbidity, mortality, tumor growth and potential macroscopic adverse effects of drug treatment. Body weight and tumor volumes were determined three

times weekly. The latter was determined in two dimensions using a caliper, and the volume was expressed in mm^3 using the formula:

$$V = 0.5 * a * b^2$$

where *a* and *b* are the long and short diameters of the tumor. All mice were terminated on day 45 after the tumor inoculation, when the excised tumor was weighted. BALB/c nude mice were from Shanghai Lingchang Bio-Technology Co. Ltd.

Ethic Statement: All animal procedures were approved by the Institutional Animal Care and Use Committee (IACUC) of CrownBio. Care and use of animals was in accordance with the regulations of the Association for Assessment and Accreditation of Laboratory Animal Care (AAALAC).

ASSOCIATED CONTENT

Supporting Information

Supporting information is available at http://pubs.acs.org

Affinity of compound **6**, selected PI3K and mTOR inhibitors to PI3K and related kinases (Table S1); Compounds investigating binding mode of **6** in PI3K and mTOR (Table S2); X-ray structure of compound **6** (Figure S1); X-Ray crystallography data collection and refinement statistics (Table S3); Modelling of **6** and compound **66** in mTOR (Figure S2); Wortmannin competition assay (Figure S3); TREEspot™ visualization of KINOMEScan interactions of PI3K/mTOR inhibitors (Figure S4); Kinase interactions (KINOMEscan™) of **6** and reference compounds (Table S4); Impact on cell proliferation of **6** and GDC0980 (**3**, Table S5); Cell growth dose response curves (Figure S5); Correlation of cellular growth inhibition profiles of **6**, **3**, and BEZ235 (Figure S6); Comparison of PQR530 (**6**) and PQR309 (**5**) efficacy on cell viability (Figure S7). Comparison of PQR530 (**6**) and PQR309 (**5**) Comparative PK in mice (Figure S8); *In vitro* pharmacology I – ligand binding assays with **6** (10 μM; Table S6); *In vitro* pharmacology II – enzyme assays with **6** at 10 μM (Table S7); PAMPA assay (Table S8A), MDCK permeability, and sensitivity to P-gp inhibitor (cyclosporine A; Table S8B); Unspecific brain tissue binding, rat (Table S8C); Safety profile of compound **6** (Table S9); NMR spectra, MALDI-MS spectra, NSI-HRMS spectra and HPLC chromatograms; Collected chemical formulas; Additional reference.

Accession Codes

The coordinates of compound PQR530 (**6**) bound to the PI3Kα catalytic subunit p110α have been deposited with PDB ID code 6OAC at wwpdb.org and rcsb.org. Authors will release the atomic coordinates and experimental data upon article publication. PDB code 5OQ4 was used for docking of compound **6** and **66** into PI3Kγ. PDB code 4JT6 was used for docking of compound **6** and **66** into mTOR kinase.

AUTHOR INFORMATION

Corresponding Author

Matthias P. Wymann, Phone: +41 61 207 5046. Fax: +41 61 207 3566.

E-mail: Matthias.Wymann@UniBas.CH

Notes: conflicts of interest

FB, PHe, PHi, and DF are current or past employees of PIQUR Therapeutics AG, Basel; and PHe, DF, and MPW are shareholders of PIQUR Therapeutics AG.

ACKNOWLEGEMENTS

We thank A. Pfaltz, R.A. Ettlin, W. Dieterle, S. Mukherjee, J. Mestan and M. Lang for advice and discussions; S. Bünger and A. Dall'Asen for technical assistance; E. Teillet, J.-B. Langlois, A. Fournier, F. Imeri, T. Masson and J. Schwarte for early synthetic efforts; we are grateful to G. Zaman and the NTRC team for help and expertise with high content screening assays.

Funding Sources

This work was supported by the Swiss Commission for Technology and Innovation (CTI) by PFLS-LS grants 14032.1, 15811.2, and 17241.1; the Stiftung für Krebsbekämpfung grant 341, Swiss National Science Foundation grants 310030_153211 and 316030_133860 (to MPW), and 310030B_138659; and in part by European Union's Horizon 2020 research and innovation programme under the Marie Skłodowska-Curie grant agreement 675392 (to MPW); by the Cancer Research Society grant CRS-22641 (to JEB).

ABBREVIATIONS USED

DIPEA, *N*,*N*-diisopropylethylamine

PK, pharmacokinetic

PI3K, phosphoinositide 3-kinase

PTEN, phosphatase and tensin homolog

PKB/Akt, protein kinase B

mTOR, mechanistic or mammalian target of rapamycin

S6K, S6 kinase

TORC, TOR complex 1 or 2

TR-FRET, time-resolved Förster resonance energy transfer

TSC2, tuberin, tuberous sclerosis 2

REFERENCES

(1) a) Wymann, M. P., Schneiter, R. Lipid signalling in disease. *Nat Rev Mol Cell Biol* **2008**, *9*, *162-176*.; b) Thorpe, L. M., Yuzugullu, H., Zhao, J. J. PI3K in cancer: divergent roles of isoforms, modes of activation and therapeutic targeting. *Nat Rev Cancer* **2015**, *15*, *7-24*.; c) Shimobayashi, M., Hall, M. N. Making new contacts: the mTOR network in metabolism and signalling crosstalk. *Nat Rev Mol Cell Biol* **2014**, *15*, *155-162*.; d) Saxton, R. A., Sabatini, D. M. mTOR Signaling in growth, metabolism, and disease. *Cell* **2017**, *168*, *960-976*.

(2) Janku, F., Yap, T. A., Meric-Bernstam, F. Targeting the PI3K pathway in cancer: are we making headway. *Nat Rev Clin Oncol* **2018**, *15*, *273-291*.

(3) Laplante, M., Sabatini, D. M. mTOR signaling in growth control and disease. *Cell* **2012**, *149*, *274-293*.

(4) a) Sarbassov, D. D., Guertin, D. A., Ali, S. M., Sabatini, D. M. Phosphorylation and regulation of Akt/PKB by the rictor-mTOR complex. *Science* **2005**, *307*, *1098-1101*.; b) Gao, T., Furnari, F., Newton, A. C. PHLPP: a phosphatase that directly dephosphorylates Akt, promotes apoptosis, and suppresses tumor growth. *Mol Cell* **2005**, *18*, *13-24*.

(5) Marone, R., Erhart, D., Mertz, A. C., Bohnacker, T., Schnell, C., Cmiljanovic, V., Stauffer, F., Garcia-Echeverria, C., Giese, B., Maira, S. M., Wymann, M. P. Targeting melanoma with dual phosphoinositide 3-kinase/mammalian target of rapamycin inhibitors. *Mol Cancer Res* **2009**, *7*, *601-613*.

(6) Maira, S. M., Stauffer, F., Brueggen, J., Furet, P., Schnell, C., Fritsch, C., Brachmann, S., Chene, P., De Pover, A., Schoemaker, K., Fabbro, D., Gabriel, D., Simonen, M., Murphy, L., Finan, P., Sellers, W., Garcia-Echeverria, C. Identification and characterization of NVP-BEZ235, a new orally available dual

phosphatidylinositol 3-kinase/mammalian target of rapamycin inhibitor with potent in vivo antitumor activity. *Mol Cancer Ther* **2008**, *7*, *1851-1863*.

(7) Serra, V., Markman, B., Scaltriti, M., Eichhorn, P. J., Valero, V., Guzman, M., Botero, M. L., Llonch, E., Atzori, F., Di Cosimo, S., Maira, M., Garcia-Echeverria, C., Parra, J. L., Arribas, J., Baselga, J. NVP-BEZ235, a dual PI3K/mTOR inhibitor, prevents PI3K signaling and inhibits the growth of cancer cells with activating PI3K mutations. *Cancer Res* **2008**, *68*, *8022-8030*.

(8) Pongas, G., Fojo, T. BEZ235: When promising science meets clinical reality. *Oncologist* **2016**, *21*, *1033-1034*.

(9) Bohnacker, T., Prota, A. E., Beaufils, F., Burke, J. E., Melone, A., Inglis, A. J., Rageot, D., Sele, A. M., Cmiljanovic, V., Cmiljanovic, N., Bargsten, K., Aher, A., Akhmanova, A., Díaz, J. F., Fabbro, D., Zvelebil, M., Williams, R. L., Steinmetz, M. O., Wymann, M. P. Deconvolution of buparlisib's mechanism of action defines specific PI3K and tubulin inhibitors for therapeutic intervention. *Nat Commun* **2017**, *8*, *14683*.

(10) Beaufils, F., Cmiljanovic, N., Cmiljanovic, V., Bohnacker, T., Melone, A., Marone, R., Jackson, E., Zhang, X., Sele, A., Borsari, C., Mestan, J., Hebeisen, P., Hillmann, P., Giese, B., Zvelebil, M., Fabbro, D., Williams, R. L., Rageot, D., Wymann, M. P. 5-(4,6-Dimorpholino-1,3,5-triazin-2-yl)-4-(trifluoromethyl)pyridin-2-amine (PQR309), a potent, brain-penetrant, orally bioavailable, pan-class I PI3K/mTOR inhibitor as clinical candidate in oncology. *J Med Chem* **2017**, *60*, *7524-7538*.

(11) Tarantelli, C., Gaudio, E., Arribas, A. J., Kwee, I., Hillmann, P., Rinaldi, A., Cascione, L., Spriano, F., Bernasconi, E., Guidetti, F., Carrassa, L., Pittau, R. B., Beaufils, F., Ritschard, R., Rageot, D., Sele, A., Dossena, B., Rossi, F. M., Zucchetto, A., Taborelli, M., Gattei, V., Rossi, D., Stathis, A., Stussi, G., Broggini, M., Wymann, M. P., Wicki, A., Zucca, E., Cmiljanovic, V., Fabbro, D., Bertoni, F. PQR309 is a novel dual PI3K/mTOR inhibitor with preclinical antitumor activity in lymphomas as a single agent and in combination therapy. *Clin Cancer Res* **2018**, *24*, *120-129*.

(12) a) Furet, P., Guagnano, V., Fairhurst, R. A., Imbach-Weese, P., Bruce, I., Knapp, M., Fritsch, C., Blasco, F., Blanz, J., Aichholz, R., Hamon, J., Fabbro, D., Caravatti, G. Discovery of NVP-BYL719 a potent and selective phosphatidylinositol-3 kinase alpha inhibitor selected for clinical evaluation. *Bioorg Med Chem Lett* **2013**, *23*, *3741-3748*.; b) Fritsch, C., Huang, A., Chatenay-Rivauday, C., Schnell, C., Reddy, A., Liu, M., Kauffmann, A., Guthy, D., Erdmann, D., De Pover, A., Furet, P., Gao, H., Ferretti, S., Wang, Y., Trappe, J., Brachmann, S. M., Maira, S. M., Wilson, C., Boehm, M., Garcia-Echeverria, C., Chene, P.,

Wiesmann, M., Cozens, R., Lehar, J., Schlegel, R., Caravatti, G., Hofmann, F., Sellers, W. R. Characterization of the novel and specific PI3Kalpha inhibitor NVP-BYL719 and development of the patient stratification strategy for clinical trials. *Mol Cancer Ther* **2014**, *13*, *1117-1129*.

(13) Sutherlin, D. P., Bao, L., Berry, M., Castanedo, G., Chuckowree, I., Dotson, J., Folks, A., Friedman, L., Goldsmith, R., Gunzner, J., Heffron, T., Lesnick, J., Lewis, C., Mathieu, S., Murray, J., Nonomiya, J., Pang, J., Pegg, N., Prior, W. W., Rouge, L., Salphati, L., Sampath, D., Tian, Q., Tsui, V., Wan, N. C., Wang, S., Wei, B., Wiesmann, C., Wu, P., Zhu, B. Y., Olivero, A. Discovery of a potent, selective, and orally available class I phosphatidylinositol 3-kinase (PI3K)/mammalian target of rapamycin (mTOR) kinase inhibitor (GDC-0980) for the treatment of cancer. *J Med Chem* **2011**, *54*, *7579-7587*.

(14) Burger, M. T., Pecchi, S., Wagman, A., Ni, Z. J., Knapp, M., Hendrickson, T., Atallah, G., Pfister, K., Zhang, Y., Bartulis, S., Frazier, K., Ng, S., Smith, A., Verhagen, J., Haznedar, J., Huh, K., Iwanowicz, E., Xin, X., Menezes, D., Merritt, H., Lee, I., Wiesmann, M., Kaufman, S., Crawford, K., Chin, M., Bussiere, D., Shoemaker, K., Zaror, I., Maira, S. M., Voliva, C. F. Identification of NVP-BKM120 as a potent, selective, orally bioavailable class I PI3 kinase inhibitor for treating cancer. *ACS Med Chem Lett* **2011**, *2*, *774-779*.

(15) Wicki, A., Brown, N., Xyrafas, A., Bize, V., Hawle, H., Berardi, S., Cmiljanović, N., Cmiljanović, V., Stumm, M., Dimitrijević, S., Herrmann, R., Prêtre, V., Ritschard, R., Tzankov, A., Hess, V., Childs, A., Hierro, C., Rodon, J., Hess, D., Joerger, M., von Moos, R., Sessa, C., Kristeleit, R. First-in human, phase 1, dose-escalation pharmacokinetic and pharmacodynamic study of the oral dual PI3K and mTORC1/2 inhibitor PQR309 in patients with advanced solid tumors (SAKK 67/13). *Eur J Cancer* **2018**, *96*, *6-16*.

(16) Fabian, M. A., Biggs, W. H., Treiber, D. K., Atteridge, C. E., Azimioara, M. D., Benedetti, M. G., Carter, T. A., Ciceri, P., Edeen, P. T., Floyd, M., Ford, J. M., Galvin, M., Gerlach, J. L., Grotzfeld, R. M., Herrgard, S., Insko, D. E., Insko, M. A., Lai, A. G., Lélias, J. M., Mehta, S. A., Milanov, Z. V., Velasco, A. M., Wodicka, L. M., Patel, H. K., Zarrinkar, P. P., Lockhart, D. J. A small molecule-kinase interaction map for clinical kinase inhibitors. *Nat Biotechnol* **2005**, *23*, *329-336*.

(17) Rageot, D., Bohnacker, T., Melone, A., Langlois, J. B., Borsari, C., Hillmann, P., Sele, A. M., Beaufils, F., Zvelebil, M., Hebeisen, P., Löscher, W., Burke, J., Fabbro, D., Wymann, M. P. Discovery and preclinical characterization of 5-[4,6-Bis({3-oxa-8-azabicyclo[3.2.1]octan-8-yl})-1,3,5-triazin-2-yl]-4-(difluoromethyl)pyridin-2-amine (PQR620), a highly potent and selective mTORC1/2 inhibitor for cancer and neurological disorders. *J Med Chem* **2018**, *61*, *10084-10105*.

(18) Brandt, C., Hillmann, P., Noack, A., Römermann, K., Öhler, L. A., Rageot, D., Beaufils, F., Melone, A., Sele, A. M., Wymann, M. P., Fabbro, D., Löscher, W. The novel, catalytic mTORC1/2 inhibitor PQR620 and the PI3K/mTORC1/2 inhibitor PQR530 effectively cross the blood-brain barrier and increase seizure threshold in a mouse model of chronic epilepsy. *Neuropharmacology* **2018**, *140*, *107-120*.

(19) Arcaro, A., Wymann, M. P. Wortmannin is a potent phosphatidylinositol 3-kinase inhibitor: the role of phosphatidylinositol 3,4,5-trisphosphate in neutrophil responses. *Biochem J* **1993**, *296*, *297-301*.

(20) a) Wymann, M. P., Bulgarelli-Leva, G., Zvelebil, M. J., Pirola, L., Vanhaesebroeck, B., Waterfield, M. D., Panayotou, G. Wortmannin inactivates phosphoinositide 3-kinase by covalent modification of Lys-802, a residue involved in the phosphate transfer reaction. *Mol Cell Biol* **1996**, *16*, *1722-1733*.; b) Stoyanova, S., Bulgarelli-Leva, G., Kirsch, C., Hanck, T., Klinger, R., Wetzker, R., Wymann, M. P. Lipid kinase and protein kinase activities of G-protein-coupled phosphoinositide 3-kinase gamma: structure-activity analysis and interactions with wortmannin. *Biochem J* **1997**, *324*, *489-495*.

(21) Engelman, J. A., Chen, L., Tan, X., Crosby, K., Guimaraes, A. R., Upadhyay, R., Maira, M., McNamara, K., Perera, S. A., Song, Y., Chirieac, L. R., Kaur, R., Lightbown, A., Simendinger, J., Li, T., Padera, R. F., Garcia-Echeverria, C., Weissleder, R., Mahmood, U., Cantley, L. C., Wong, K. K. Effective use of PI3K and MEK inhibitors to treat mutant Kras G12D and PIK3CA H1047R murine lung cancers. *Nat Med* **2008**, *14*, *1351-1356*.

(22) a) Khan, K. H., Wong, M., Rihawi, K., Bodla, S., Morganstein, D., Banerji, U., Molife, L. R. Hyperglycemia and phosphatidylinositol 3-kinase/protein kinase B/mammalian target of rapamycin (PI3K/AKT/mTOR) inhibitors in phase I trials: incidence, predictive factors, and management. *Oncologist* **2016**, *21*, *855-860*.; b) Hopkins, B. D., Pauli, C., Du, X., Wang, D. G., Li, X., Wu, D., Amadiume, S. C., Goncalves, M. D., Hodakoski, C., Lundquist, M. R., Bareja, R., Ma, Y., Harris, E. M., Sboner, A., Beltran, H., Rubin, M. A., Mukherjee, S., Cantley, L. C. Suppression of insulin feedback enhances the efficacy of PI3K inhibitors. *Nature* **2018**, *560*, *499-503*.

(23) Thelen, M., Wymann, M. P., Langen, H. Wortmannin binds specifically to 1-phosphatidylinositol 3-kinase while inhibiting guanine nucleotide-binding protein-coupled receptor signaling in neutrophil leukocytes. *Proc Natl Acad Sci U S A* **1994**, *91*, *4960-4964*.

(24) Chen, P., Deng, Y. L., Bergqvist, S., Falk, M. D., Liu, W., Timofeevski, S., Brooun, A. Engineering of an isolated p110α subunit of PI3Kα permits crystallization and provides a platform for structure-based drug design. *Protein Sci* **2014**, *23*, *1332-1340*.

(25) Kabsch, W. XDS. *Acta Crystallogr D Biol Crystallogr* **2010**, *66*, *125-132*.

(26) McCoy, A. J., Grosse-Kunstleve, R. W., Adams, P. D., Winn, M. D., Storoni, L. C., Read, R. J. Phaser crystallographic software. *J Appl Crystallogr* **2007**, *40*, *658-674*.

(27) Emsley, P., Lohkamp, B., Scott, W. G., Cowtan, K. Features and development of Coot. *Acta Crystallogr D Biol Crystallogr* **2010**, *66*, *486-501*.

(28) Afonine, P. V., Grosse-Kunstleve, R. W., Echols, N., Headd, J. J., Moriarty, N. W., Mustyakimov, M., Terwilliger, T. C., Urzhumtsev, A., Zwart, P. H., Adams, P. D. Towards automated crystallographic structure refinement with phenix.refine. *Acta Crystallogr D Biol Crystallogr* **2012**, *68*, *352-367*.

(29) Chen, V. B., Arendall, W. B., Headd, J. J., Keedy, D. A., Immormino, R. M., Kapral, G. J., Murray, L. W., Richardson, J. S., Richardson, D. C. MolProbity: all-atom structure validation for macromolecular crystallography. *Acta Crystallogr D Biol Crystallogr* **2010**, *66*, *12-21*.

(30) Karaman, M. W., Herrgard, S., Treiber, D. K., Gallant, P., Atteridge, C. E., Campbell, B. T., Chan, K. W., Ciceri, P., Davis, M. I., Edeen, P. T., Faraoni, R., Floyd, M., Hunt, J. P., Lockhart, D. J., Milanov, Z. V., Morrison, M. J., Pallares, G., Patel, H. K., Pritchard, S., Wodicka, L. M., Zarrinkar, P. P. A quantitative analysis of kinase inhibitor selectivity. *Nat Biotechnol* **2008**, *26*, *127-132*.

(31) Kumar, N., Khan, S. I., Rawat, D. S. Synthesis and antimalarial-activity evaluation of tetraoxane triazine hybrids and spiro [piperidine-4,3′-tetraoxanes]. *Helvetica Chimica Acta* **2012**, *95*, *1181-1197*.

(32) Kumar, A., Srivastava, K., Kumar, S. R., Siddiqi, M. I., Puri, S. K., Sexana, J. K., Chauhan, P. M. 4-Anilinoquinoline triazines: a novel class of hybrid antimalarial agents. *Eur J Med Chem* **2011**, *46*, *676-690*.

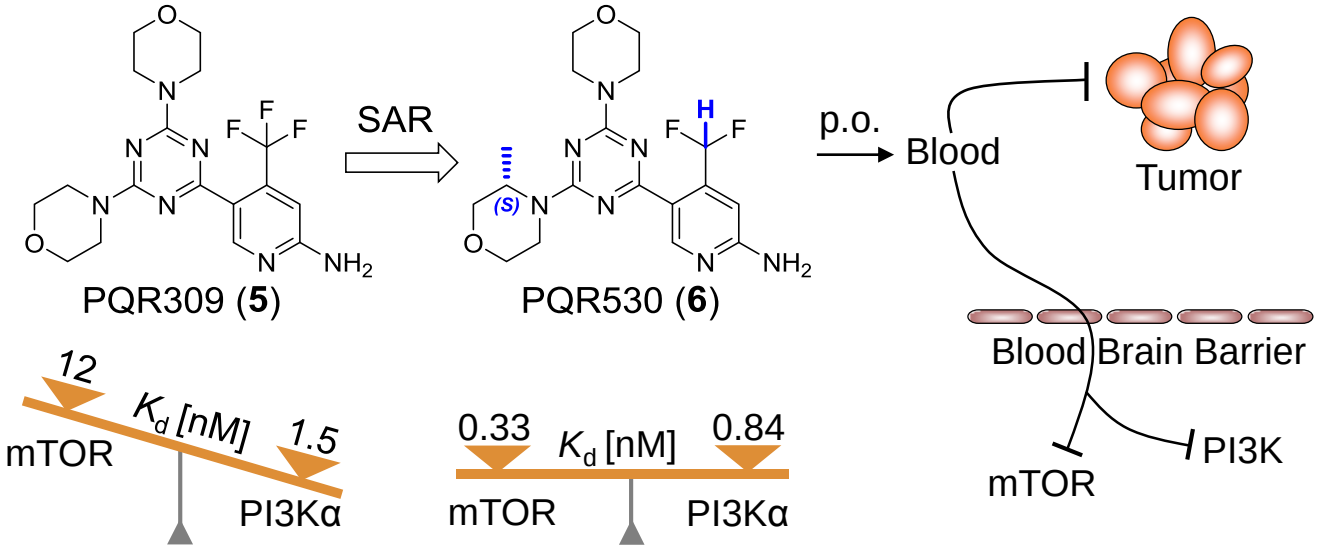
SAR
PQR309 (5)
PQR530 (6)
p.o.
Blood
Tumor
Blood Brain Barrier
PI3K
mTOR
12
Kd [nM]
1.5
mTOR
PI3Kα
0.33
Kd [nM]
0.84
mTOR
PI3Kα